ABSTRACT

Shane Cecil Clark, Development of P-y curves for a Well Graded Gravel. (Under the direction of Dr. Mohammed Gabr and Dr. Roy Borden)

Research work is conducted to investigate the possibility of using laboratory model tests to simulate lateral response of drilled shafts embedded in soft weathered rock and discern their P-y curve function. Eight lateral load tests on instrumented model piles embedded in an Aggregate Base Course (ABC) medium are performed to evaluate the P-y curves. The ABC material is selected to simulate the response of soft weathered rock encountered in the field. The laboratory-evaluated P-y curves are compared to data from full-scale field tests performed in weathered rock. The two key parameters evaluated are the modulus of subgrade reaction (k_{ho}) and the ultimate lateral resistance (P_{ult}). Using the laboratory-measured data, in comparison to measured field behavior, correlations for the subgrade modulus as a function of depth, as well as simplified approximations of P_{ult} are developed for weathered rock materials. Results indicated that a hyperpolic P-y function seems to best represent the measured laboratory P-y curves. A comparison between laboratory and field data indicated that the ABC testing medium appears to yield k_{ho} and P_{ult} that behave in a fashion similar to weathered rock material. Accordingly, it seems that, when appropriately mixed, that ABC can be used to model SWR encountered in the field. A distribution of k_{ho} with applied confining stress is evaluated and compared to results from procedures proposed by Reese (1997) for weathered rock and Terzaghi (1955) for stiff clay. A relationship developed for the distribution of subgrade modulus as a function of depth compared well with field data. The relationship of P_{ult} with depth as a function of Geological Strength Index (GSI) and friction angle is also presented. All results are viewed in the context of the field measured response.

DEVELOPMENT OF P-Y CURVES FOR A WELL GRADED GRAVEL

by

SHANE C. CLARK

A thesis submitted to the Graduate Faculty of
North Carolina State University
In partial fulfillment of the
Requirements for the Degree of Master of Science

CIVIL ENGINEERING

Raleigh

2001

APPROVED BY:

_____

_____ _____

Chair of Advisory Committee Co-Chair of Advisory Committee

BIOGRAPHY

Shane Cecil Clark was born on October 24, 1967, in Shelby, North Carolina. He grew up in Hickory, North Carolina, and attended elementary, junior high, and high school there. In 1986 after graduating high school, he moved to Asheville, North Carolina to attend the University of North Carolina at Asheville. In December 1992, he graduated with a B.S. in Environmental Science. In September 1995, Shane married Kelly A. Pippinger. After a brief career in wastewater treatment, Shane and Kelly decided to take advantage of their youth and opportunity, in the form of traveling around the United States for 10 months. During this time, they were able to visit 22 states and cover 24,000 miles connecting them. Shortly upon returning to Asheville, Shane decided to pursue a degree in Civil Engineering, which culminated in a December 1999 graduation from North Carolina State University. After completion of this degree, he decided to further his education in Geotechnical Engineering and obtained a Master's of Science in Civil Engineering in 2001 from North Carolina State University.

ACKNOWLEDGEMENTS

The author would like to thank the following individuals for the roles they played in his education and completion of this project.

Dr. Mohammed Gabr for his guidance and confidence in my abilities. You have truly provided all that was needed for me to attain my goals.

Dr. Roy Borden for helping to fine tune my thinking and analysis processes. I feel I have learned a lot from you both on an academic as well as a personal level.

Dr. Shamimur Rahman for taking interest in my thesis work and reviewing my thesis.

Kook Hwan Cho for helping with all aspects of this project and clarifying my sometimes cloudy thinking. I have enjoyed getting to know you and look forward to future friendship. Best of Luck with your Ph.D.

Jodie Nixon and Jun Hoon Kim for their assistance with testing.

Lastly and most importantly, to Kelly, my companion, friend, and wife, for your unending patience and support, Thank You.

TABLE OF CONTENTS

Page No.

LIST OF FIGURES

LIST OF TABLES

1.0 INTRODUCTION

Background

Deep foundations, such as those involving drilled shafts and piles, are used in a number of civil engineering projects. These include supporting buildings, bridges, towers as well as other highway and domestic structures. Deep foundations generally involve two types of support. The first is in the form of vertical, or axial, support. This is accomplished through a combination of side shear resistance and end bearing. The second form of support is through lateral resistance. Lateral resistance is necessary to overcome loadings induced by earth pressures, wind forces, earthquakes, and centrifugal forces from moving vehicles, for example. Often, in design, the lateral resistance governs the final length of the piles, or shafts, and thus the cost of the foundation. Lateral resistance of piles has been thoroughly researched for sand and clays, and several published methods exist for their analysis (e.g. Reese et al., 1974 and Matlock 1970). However, limited data involving rock and weathered rock profiles are available in literature.

In locations where geologic discontinuities have resulted in relatively soft soils overlying massive hard rock, the geometry of the soil-rock boundary can be reasonably defined with existing subsurface exploratory techniques. In areas of weathered and decomposed rock profiles, such as that of the Piedmont Physiographic province of the southeastern United States, definition of the soil-rock boundary is a recurring challenge for engineers and contractors. In this situation, the subsurface conditions typically consist of surface soils derived from extensive weathering of the parent rock. With depth, the soils grade into less-weathered material and more evidence of the parent rock features are retained. At some depth, virtually no signs of weathering within the rock

mass can be detected. Quantitative definitions of the soil-rock interface have been addressed in the literature. For example, Coates (1970) recommended that the Rock Quality Designation (RQD) value could be used to estimate depth to sound rock. RQD values smaller than 25% designate very poor rock quality that could be classified as soil for engineering purposes. The RQD is defined as the percent of the coring interval represented in the core box by sound, unweathered cylinders at least 4 inches in length. Peck (1976) stated that the distinction between rock-like and soil-like material in transition zones is usually unpredictable. Figure 1, presented by Kulhawy et al (1991) shows the depiction of different residual profiles based on the definition of different researchers.

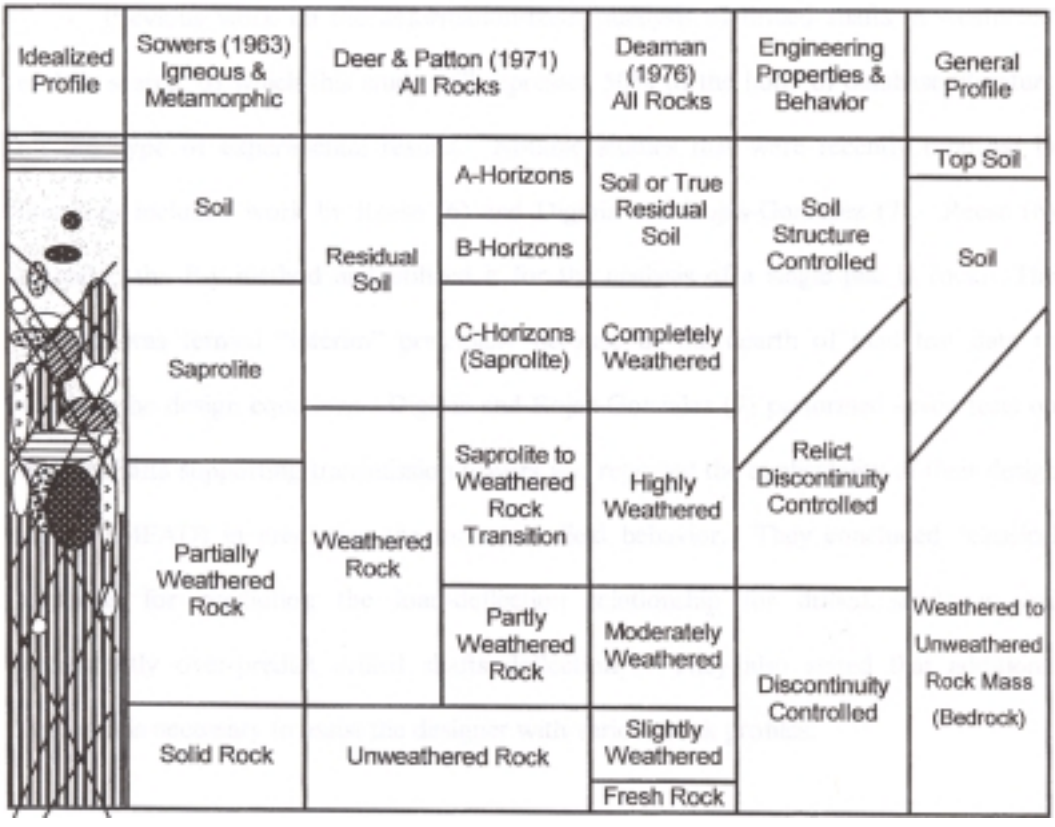

Figure 1 Residual Profiles based on definition (Kulhawy et al., 1991).

In these types of transitional subsurface profiles, the definition of the soil parameters needed for the analysis and design of laterally loaded drilled shafts poses a great challenge for engineers and contractors. The lack of an acceptable analysis procedure is compounded by the unavailability of a means for evaluating the weathered profile properties, including the lateral rock modulus, which often leads to the over design (conservative) of the shaft foundation. Given that the cost of shaft construction in rock is on the order of $1500 per meter length for a shaft that is one and a half meters in diameter, $1.5 million dollars of savings for every 1000 shafts can be realized if the depth of embedment is reduced by 1 meter, while maintaining acceptable and safe performance. This substantial cost saving could be realized if a rational method for the analysis and design of shafts in soft and weathered rock profiles is developed (Keaney, 2000).

As presented by Gabr and Borden (1992) and Gabr (1993) a deformation-based definition of the factor of safety for laterally loaded shafts can lead into economic and safe design as long as variability in soil and rock properties and applied loads are taken into account. The three most common deformation-based analytical models used to obtain theoretical solutions for piles placed in deforming soils include:

i. Subgrade reaction approach based on the assumption of Winkler foundation,
ii. Linear approach based on the theory of elasticity, and,
iii. Numerical solutions using finite element, finite difference, and boundary element techniques with the soil modeled using either the subgrade or linear approach, or a combination thereof.

One of the most challenging aspects related to the determination of required drilled shaft embedment in rock is the to estimate the modulus of lateral subgrade

reaction of the soft weathered rock. A literature review yielded no documentation of research that was performed specifically to develop subsurface investigation techniques for characterizing the lateral subgrade modulus of weathered rock. Insitu investigation techniques are specially needed in this case since the profile materials are transitional between easily excavatable, adhesionless soils and massive, hard rock that is without weakened discontinuities. Since the rock in this transitional zone is decomposed, it is increasingly difficult to retrieve representative samples. Even when samples are retrieved, conventional tests preformed on intact cores do not provide representative characteristics of the lateral behavior of the rock mass layers. A relationship between the insitu and laboratory rock moduli has been presented in literature by Coon and Merrit (1970) for higher RQD rocks where the RQD is typically greater than 70%. This relationship is depicted in Figure 2. Unfortunately no such relationship exists for the highly weathered rock with lower RQD values. The weathering conditions and the inability to retrieve representative samples from the field necessitate the performance of insitu testing in order to obtain representative modulus values.

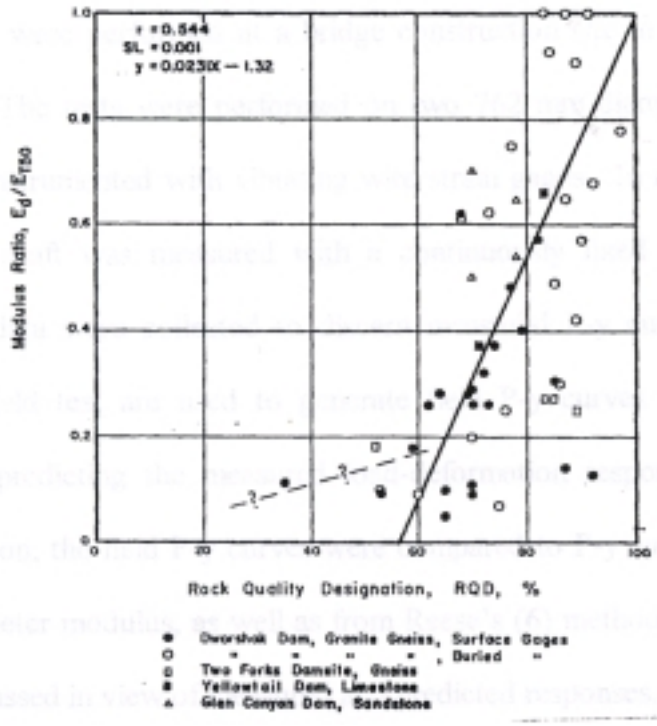

Figure 2 Comparison of RQD and the Modulus Ratio E_d/E_{t50} (Coon and Merrit, 1970).

1.2 Problem Statement

To properly model soft weathered rock under lateral loading, the properties of the materials must be evaluated. These properties are key in describing the soil-structure-interaction behavior. The work reported in this thesis is a part of a research program to develop P-y curves for drilled shafts embedded in soft weathered rock (SWR). This part of the research program is undertaken to evaluate P-y curves from model piles tested in an Aggregate Base Course (ABC) mixture. The ABC is used to represent some degree of stiffness that is indicative of the in situ weathered rock material. The ABC material is chosen for the laboratory tests due to its availability and relative ease of compaction and reuse in the testing scheme. While ABC is not in fact weathered rock, it is hypothesized that the presence of hard rock particles in combination with smaller soil-like particles

simulates, in some ways, the way weathered rock might behave under lateral loading. A major outcome of this work is comparing the field and laboratory measured behaviors and providing data regarding the ability to use ABC material to simulate SWR in the filed.

1.3 Objectives

The main objective of this study is to evaluate P-y curves from laboratory model pile tests in gravelly soils. The resulting P-y curves and associated behavior of the soil-pile interaction are compared to full-scale field tests in weathered rock profiles. These comparisons will be used to further study and develop a complete P-y curve model for drilled shafts embedded in soft weathered rock profiles. The following specific objectives are pursued in this study:

1. Development of a representative lateral loading test method in the laboratory,
2. Development of a trend function describing the laboratory-measured P-y curves in the ABC material,
3. Estimate the variation of measured key parameters, k_{ho} and P_{ult}, as a function of confining stress,
4. Determine P-y curves for the soil being tested and compare the results to full-scale load test results in weathered rock, and,
5. Provide conclusion regarding the suitability of using ABC material to simulate soft weathered rock material.

The results of the laboratory tests, under controlled conditions, will be used to define the shape of the P-y curves. In addition, the resulting P-y curves from laboratory tests will be

used in a future study to verify F.E.M. modeling that was performed for the laboratory testing. Accordingly, the laboratory testing and modeling will provide validity to field modeling which is currently underway to determine field failure planes. (Personal communication, Cho, 2001)

2.0 LITERATURE REVIEW

Past work on the deformation-based analysis of drilled shafts in weathered rock is scarce. Notable studies that were recently reported in literature include work by Reese (1997) and Digioia and Rojas-Gonzalez (1994). Reese (1997) extended the P-y method and utilized it for the analysis of a single pile in rock. The method was termed "interim" principally because of the dearth of load test data to validate the design equations. Digioia and Rojas-Gonzalez (1994) performed seven tests on drilled shafts supporting transmission towers and reported the applicability of their design model (MFAD) in predicting the measured field behavior. They have concluded "classical methods for the prediction of the load-deflection relationship for drilled shafts in soil consistently over-predict drilled shaft deflection." They also stated that additional research was still necessary to assist designers facing rock profiles.

Two methods of insitu testing can possibly be used to measure lateral insitu modulus values. The first method is commonly referred to as a plate-jacking test. The plate-jacking test requires excavating a trench from grade to desired testing depth. A hydraulic ram and deformation measuring instruments are placed in the trench. The ram is used to provide a measurable force against the sides of the trench from which deformation is induced and measured. Obviously, performing such a test at a depth greater than perhaps 1.0 m is challenging and cost prohibitive due to the magnitude of required shoring and excavation.

The second emerging method is based on using a borehole dilatometer (referred to as a rock dilatometer model Probex 1.) The borehole dilatometer (manufactured by ROCTEST, Plattsburgh, NY) is a specialized probe that uses an expandable bladder to

apply force to the walls of an N-size borehole. Volume change of the probe under stress increments is measured at the probe level. Lateral rock modulus can be derived based on the pressure-volume measurements in a manner similar to that employed for the pressuremeter test (PMT). The rock dilatometer can be used at the time the subsurface investigation is performed at a given site to estimate the insitu lateral modulus of the rock as a function of depth. The maximum working pressure that can be applied is 30,000 kPa (4350 psi), according to the manufacturer literature.

Once the pressure and corresponding volume change values have been attained, they can be used to predict the lateral loading behavior. In order to accurately model this behavior, testing in a controlled environment is needed. According to Mayne et al., as of 1995, there have been approximately 49 model studies to determine the effects of lateral loading. Additional review found no testing programs that involved gravelly soils, such as ABC. Additionally, the author found several methods of instrumentation for the model piles and/or shafts. This information was used to form the general direction of this research.

2.1 Background on P-y Analysis Method

Single piles and pile groups are frequently subjected to high lateral forces. These lateral forces may be caused by earthquakes, by wave or wind forces or lateral earth pressures due to slope instability.

When a pile is laterally loaded the soil exerts a pressure against the pile and equilibrium is reached. The pressure, p (lb/in^2) varies with depth and is defined by:

$$p = k_{ho}y \quad (1)$$

where, k_{ho} is the coefficient of subgrade reaction that is normally attributed to Winkler, and y is the lateral displacement of the pile.

The simplicity of Winkler's model to evaluate the modulus of subgrade reaction, the availability of chart solutions, and ease of hand calculations favor the use of this concept to this day. The usual physical model used to depict this relationship is a series of linear spring. A P-y curve is a nonlinear version of the Winkler spring system and is calculated in terms of a pressure versus deflection curve for a finite number of points along a pile. This concept was primarily developed by Reese et al. (1974) for the analysis of laterally loaded piles.

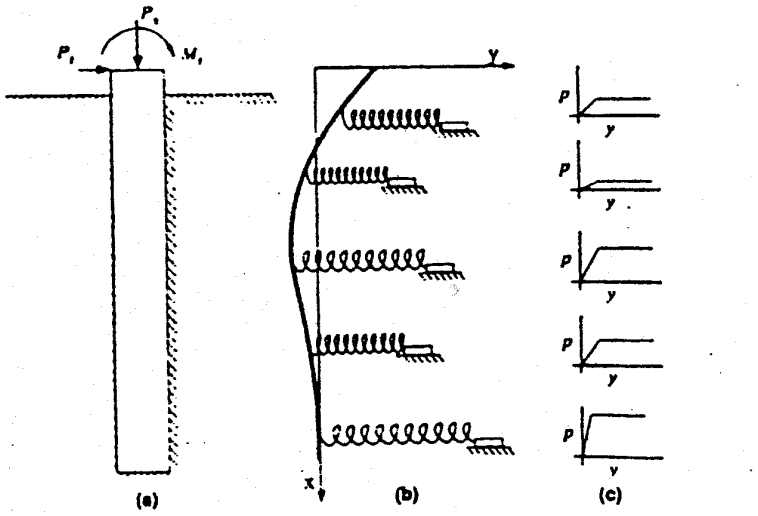

Figure 3 Winkler Spring Model

Nonlinear load-deflection analytical techniques utilizing the theory of subgrade reaction are considered most useful for the analysis of laterally loaded piles and piers. A solution based on the subgrade reaction approach requires a better understanding of soil-pile load-deflection characteristics, referred in this report as P-y curves.

When multiplying the soil pressure, p (lb/in^2), by the pile width (or diameter), the force P (lb/in) is obtained. This allows us to consider the concept of the modulus of subgrade reaction by the following expression:

$$P = k_h y \qquad (2)$$

Where, P(lb/in) = soil reaction = p y
k_h (lb/in^2) = modulus of subgrade reaction = k_{ho} y
k_{ho} (lb/in^3) = coefficient of subgrade reaction
y (in) = pile deformation

When external loadings of different magnitudes are applied, the P-y curves may be developed to show soil-pile load-deflection characteristics. P-y curves may be plotted for various depths along a pile and are considered to vary depending on the soil type as well as the pile stiffness characteristics. According to Meyerhof (1976) a free head pile in homogeneous elastic soil my be considered rigid if its relative stiffness, $K_r \geq 0.01$, where K_r is defined as:

$$K_r = \frac{E_p I_p}{E_h L^4} \qquad (3)$$

where E_p = modulus of elasticity of the pile,
I_p = moment of inertia of the pile,
E_h average horizontal modulus, k_h and,
L = length of pile.

According to Mattlock, the proper form of the P-y relation is influenced by many factors, including *(1)* natural variation of soil properties with depth, *(2)* the general form of the pile deflection, *(3)* the corresponding state of stress and strain throughout the affected soil zone, and *(4)* the rate and sequence and history of cyclic wave loading.

No matter how complex the loading becomes, to perform an analysis for design it must be possible to reduce the soil behavior at each depth to a simple P-y curve.

2.2 Piedmont Transition Zone

North Carolina's geology is divided into three distinct regions: the Coastal Plain, Piedmont, and Mountains. The coastal plain formations are comprised of limestone and undifferentiated unconsolidated materials at the surface. This area is predominately thought of as composed of sedimentary soils and rocks, due to transportation of sediments. The Piedmont and Mountain regions are geologically composed of igneous and metamorphic rocks (Horton, 1991). Over millions of years, these parent rocks have weathered into residual soils, which retain much of the fabric and many of the structural features of the original rock. The degree of weathering decreases with increasing depth, usually with no well-defined boundary between soil and rock. Although the weathering materials have the texture of soils, they retain enough of the fractures of rock that their behavior under load can often be modeled better by the methods of rock mechanics than by soil mechanics (Sowers, 1983).

Engineers often ask what is the cohesion and/or friction angle, or what is the stiffness or modulus of the material? These are legitimate questions because many engineers need to know these values to be able to design cost effective foundations. Drilled shafts are often the foundation of choice if loadings and unsupported lengths, due to scour, dictate. These foundations often must extend through the upper soils into the weathered rock and sometimes into hard rock. In some cases, shaft foundations must penetrate the hard rock layer due to little weathering below the alluvial soils, however many cases are encountered where weathered rock thickness of five (5) feet or greater lies above the hard rock. This poses very hard questions for the design engineer. What

properties should be assigned to this material when analyzing shafts for axial and lateral stability?

Often, when the design is underway, the axial stability is reached before lateral stability, thus lateral resistance often controls the final design. Therefore, properties must be assigned to this "transition zone" when analyzing with the P-y curve analysis. Soil and rock properties are the only option, therefore, conservatism must be exercised and soil properties are usually assigned to the weathered rock.

2.3 P-y Curves in Rock

There are a few published methods for determining P-y curves in rock. Generally these methods adjust strength values obtained from intact rock specimens.

2.3.1 Reese's Method

Reese (1997) proposed a method to construct P-y curves for weak rock. The resistance p_{ur} for rock is based on limit equilibrium and reflects the influence of the surface of the rock:

$$p_{ur} = \alpha_r q_{ur} b(1+1.4x_r/b); \qquad 0 \le x_r \le 3b \tag{4}$$

$$p_{ur} = 5.2\alpha_r q_{ur} b; \qquad x_r \le 3b \tag{5}$$

Where, q_{ur} = compressive strength of rock (usually lower-bound as function of depth),
α_r = strength reduction factor,
b = diameter of pile and,
x_r = depth below rock surface

If one were to consider a strip from a beam resting on an elastic, homogeneous, and isotropic solid, the initial modulus K_i (p_i divided by y_i) may have the following value:

$$K_{ir} = k_{ir} E_{ir} \tag{6}$$

Where, E_{ir} = initial modulus of rock and,
k_{ir} = dimensionless constant.

Reese (1997) suggested Equations 7 and 8 for estimating k_{ir}. These functions are derived experimentally and reflect the assumption that the presence of the rock surface will have a similar effect in k_{ir}, as was shown for p_{ur} for ultimate resistance.

$$k_{ir} = (100 + 400x_r/3b); \qquad 0 \le x_r \le 3b \tag{7}$$
$$k_{ir} = 500; \qquad x_r \ge 3b \tag{8}$$

Equations 7 and 8, developed from experimental data, show that the initial portions of the P-y curves are very stiff in order to model the relatively low deflections observed during initial loads. Further explanation is warranted for these equations. First, the equations have no influence on solutions beyond the value y_A, Figure 3, and probably will have no influence on the designs based on the ultimate bending moment of a pile. Second, available load test data, while incomplete, show much lower values of K_{ir} in relation to the modulus of rock or soil. Third, the increase in K_{ir} with depth in Equation 4 is consistent with results obtained from the lateral loading of piles in overconsolidated clays.

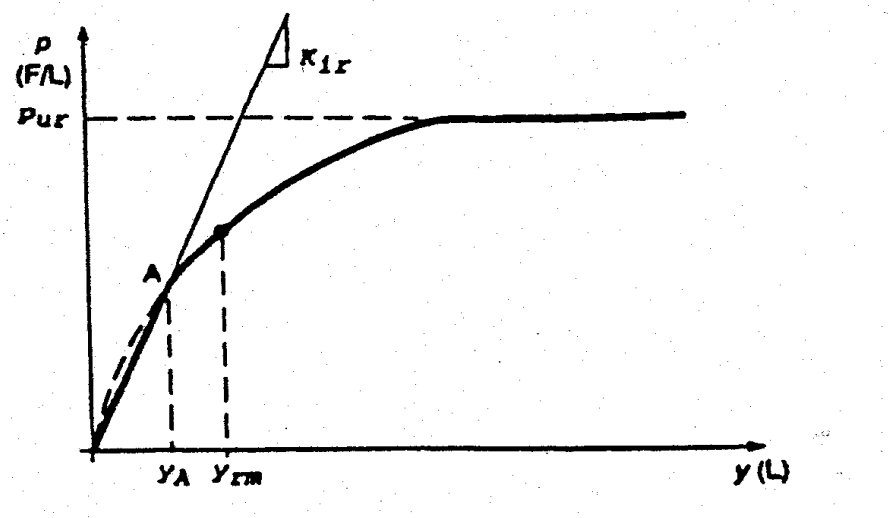

Figure 4 Influence of ya.

With guidelines for computing p_{ur} and K_{ir}, the equations for the three branches of the family of P-y curves shown in Figure 4 are as follows. The equation for the straight-line, initial portion of the curves is given by equations 9 and, for the other branches, equations 10 to 12;

$$p = K_{ir} y; \qquad y \le y_A \tag{9}$$

$$p = \frac{P_{ur}}{2}\left(\frac{y}{y_{rm}}\right)^{0.25}; \qquad y \ge y_A; \quad p \le p_{ur} \tag{10}$$

$$p = p_{ur} \tag{11}$$

$$y_{rm} = k_{rm} b \tag{12}$$

where, k_{rm} = constant, ranging from 0.0005 to 0.00005, and serves to establish the overall stiffness of the curves. The value of y_A is found by solving for the intersection of equations 9 and 10 and is shown by equation 13 below:

$$y_A = \left[\frac{p_{ur}}{2(y_{rm})^{0.25} K_{ir}}\right]^{1.333} \tag{13}$$

Equations 9 through 13 predict the behavior of single piles under lateral loadings. Using the results of two lateral load tests, Reese validated this P-y model using these equations.

2.3.2 P-y Curve Prediction by Reese, Cox, and Koop's Method

Another possible procedure for the construction of P-y curves in soft rock could be synthesized from that presented by Reese, Cox, and Koop (1975) to model P-y curves in stiff clay above groundwater. The shape of the P-y curve is generated using following equation,

$$\frac{P}{P_{ur}} = \left(\frac{y}{16 y_{50}}\right)^{\frac{1}{4}} \tag{14}$$

Comparisons of measured and predicted behavior of drilled shafts in rock performed and presented by Carter and Kulhawy (1992), were performed by Gabr (1993) using equation 15 and the data are presented in Table 1.

Table 1 Analysis Parameters used in the P-y predictions (Gabr 1993)

Shaft	E_r	q_u	ε_{50} (%)	$y_{50} = 2.5\varepsilon_{50}$ B	$y_{50} = \varepsilon_{50}$ B
Shaft 14-D	101 (MN/m^2) 14,352 (psi)	4.2 (MN/m^2) 60 (psi)	0.4	12.2 (mm) 0.5 (in.)	4.9 (mm) 0.2 (in)
Shaft 14-U	414 (MN/m^2) 58,829 (psi)	14.1 (MN/m^2) 120 (psi)	0.4	9.1 (mm) 0.4 (in.)	3.6 (mm) 0.16 (in.)

A stiffer response of P-y curve is simulated by assuming $y_{50} = \varepsilon_{50}$ B to parametrically study the effect of P-y magnitude on the predicted behavior. Predictions were performed using the computer program LTBASE by Gabr and Borden (1988).

Figure 5 shows the measured and predicted responses of the two shafts using stiffness and strength values reported in Table 1. Results indicate that better fit of the measured data was obtained using stiffness and strength data estimated at the location of 14-D with $y_{50} = \varepsilon_{50}$ B. Using E_r = 101 MN/m^2 and q_u = 4.2 MN/m^2 the monotonic non-

linear trend of displacement increase with load was approximately predicted for both shafts. On the other hand, using E_r = 414 MN/m^2 and q_u = 14.1 MN/m^2, softer responses compared to measured data were predicted assuming $y_{50} = 2.5\varepsilon_{50}$ B and stiffer responses were predicted for both shafts assuming $y_{50} = \varepsilon_{50}$ B.

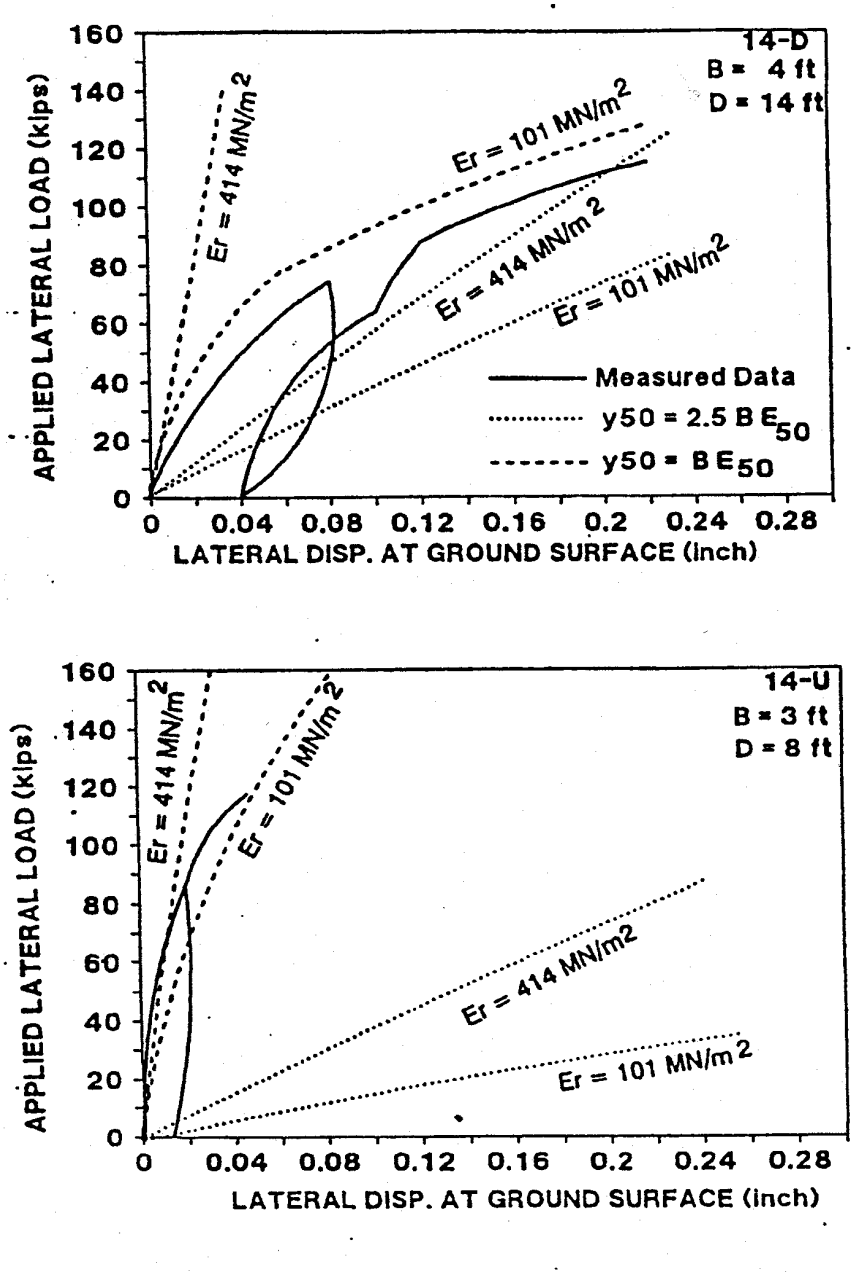

Figure 5 Predicted vs. Measured Response (Gabr, 1993).

The predicted behavior using the subgrade reaction approach is dependent on the shape and magnitude of the characterized P-y curves. These curves can be defined by the modulus of lateral subgrade reaction (k_{ho}) which is a function of E_r, and the y_{50}, which is a function of ε_{50}, and the ultimate soil resistance (P_u). Accordingly, using $y_{50} = \varepsilon_{50}$ B compared to $y_{50} = 2.5\varepsilon_{50}$ B produced a stiffer P-y response with shorter initial slope. Consequently, and by using $y_{50} = \varepsilon_{50}$ B, the non-linearity effect is more represented at the early stage of loading as shown in Fig. 5.

A comparison between Reese's Method (1997) and Reese, Cox, and Koop's method (1975), which assumes $y_{50} = \varepsilon_{50}$ B, is performed using same parameters for Shaft 14-D described in Table 1, and plotted in Fig. 5. As shown in Fig. 6, the predicted P-y curves show that the ultimate load of Reese's method (1997) at the displacement (y) of 0.008 m is almost 2 times larger than the load at the same displacement using Reese, Cox, and Koop's Method (1975). Therefore, the Reese's method (1997) can be considered overestimating P-y curves for rock, and should be used with caution.

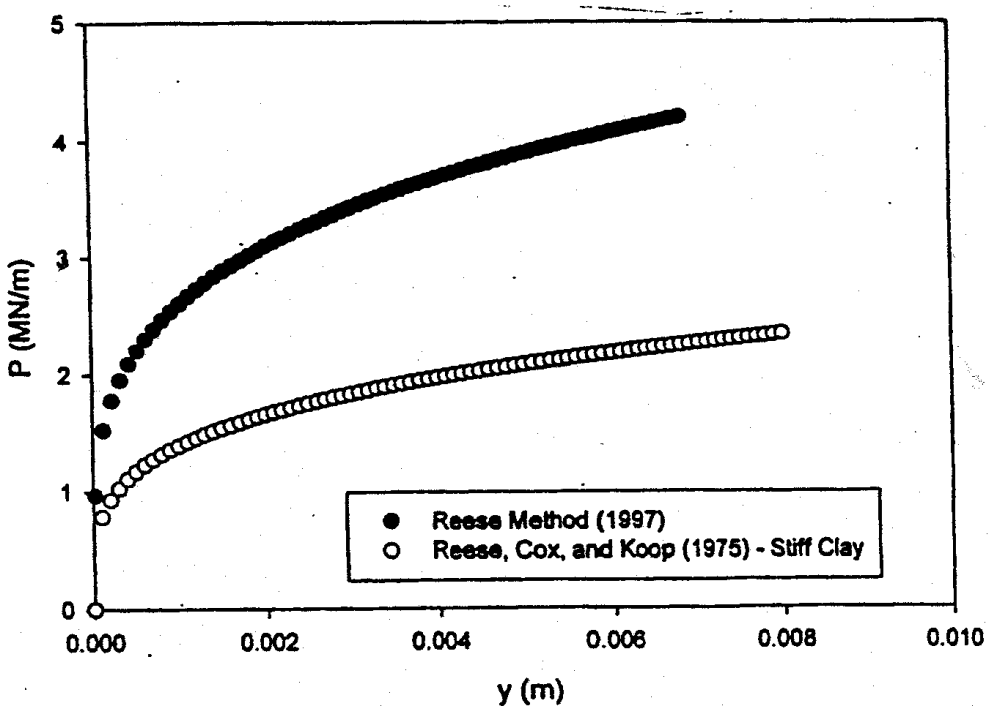

Figure 6 P-y Curve comparison.

3.0 EXPERIMENTAL PROGRAM

3.1 Laboratory Testing Program

The testing program included performing eight tests on instrumented model piles. Two were performed in sand and six were performed in an ABC mixture. The sand tests were mainly conducted to ensure that system components functioned properly and to examine and develop the testing procedures. The results of the sand testing are not reported here. Testing in the ABC mixture began in December 2000 and was completed in May 2001. A total of 6 tests were performed in the compacted ABC mixture, however only two of these tests are reported here. The remaining 4 tests have been discarded due to 1) nonhomogenous testing mix (first two tests) and instrumentation failures on the pile with short embedment (two total). Figure 7 displays the testing matrix that was employed in this study.

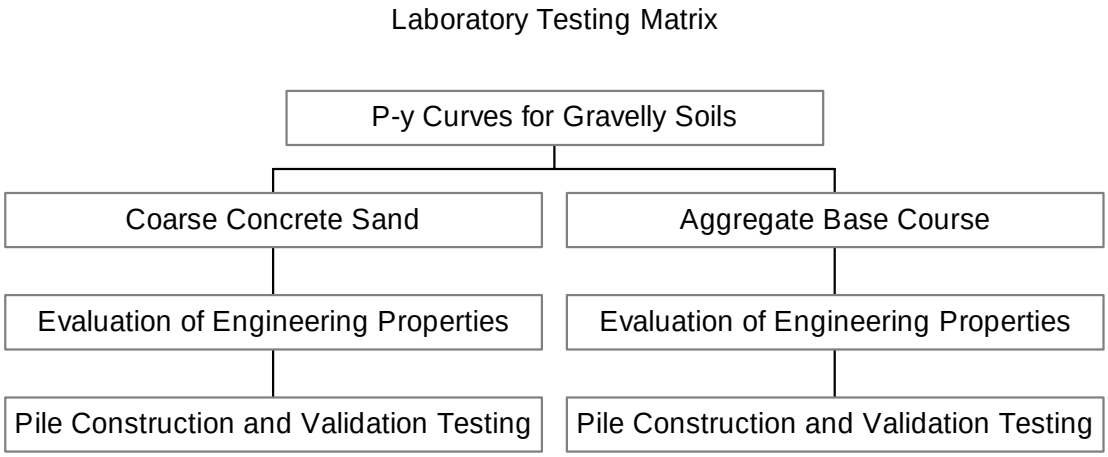

Figure 7 Testing Scheme for Laboratory Testing.

3.2 Testing Setup

The load test pit is located in the Geotechnical Testing Lab, in the Constructed Facilities Lab, on Centennial Campus. This testing area is composed of a 6 ft wide x 12 ft long x 8 ft tall concrete walled chamber as shown in Figure 8. Based on a finite element analysis, this testing chamber was deemed large enough to allow duplicate tests to be conducted without the introduction of boundary effects. This duplication allows verification of results by introducing a comparison test. To simulate overburden pressures found in the field, a combined lateral loading and surcharging system was developed for use in this chamber in order to simulate the application of different levels of confining stresses. Figure 9 shows the surcharge loading system which is comprised of the following: 1) 24 inch x 33 inch 1 inch thick A36 steel plates, two W6 x 20 x 72 inch loading members, and a W6 x 20 x 30 inch cross member. Based on a simply supported beam analysis for each component, it was estimated that the total deflection encountered would be less than 0.25 inches under a full 30-ton applied load. Based on the flexural rigidity of the loading frame, it is assumed that, if a level loading surface is provided, that the applied stress will be uniform.

The loading frame was used to attach two 30-ton hydraulic jacks that can apply load in the vertical direction. Given this capacity, this loading system is capable of applying stress simulating up to 50 feet of overburden. To monitor the actual applied load, two 50,000 pound StrainSert load cells were placed between the loading points on the jacks and the reaction beam. The load signals were measured using a Vishay P-3500 digital readout box.

Figure 8 Testing Chamber.

Figure 9 Surcharging and Lateral Loading System.

3.3 Testing Medium

Testing was conducted using an aggregate base course mixture. The proportions of this mixture were based on the analyses of boring logs and coring samples obtained from dilatometer and load test site data. Table 2 displays location of these sites as well as the measured recovery (REC) and rock type. This analysis revealed that the recovered cores averaged approximately a 30 % loss of material. This interpretation was based on a average REC of 70 %. It is assumed that the remaining 30% was finer materials that washed and/or slaked during the coring process. For our purposes, fines are defined as particles smaller than approximately 3/16 th inch (~ 4.75 mm). This value is the dividing line between sands and gravels, according to the Unified Soil Classification System.

Table 2 Rock Test Data

COUNTY	REC (%)	ROCK TYPE
AVERY	69	GNEISS
	70	
	60	
	37	
	70	
	40	
	26	
CALDWELL	93	GNEISS
	86	
WILSON	76	METAVOLCANIC
	80	
	100	
	100	
	90	
GUILFORD	61	METADIORITE
	92	
AVERAGE	~ 72.0 %	

To create an appropriate testing medium the strength and behavior characteristics must be considered. When weathered rock is encountered in the field, it generally consists of larger rock particles on the order of 2~4 inches and then grades down to a mixture of fines. The actual composition is a function of the rock type and degree of weathering as noted in the variations of %REC in Table 2, above. Thus, it was rationalized that our simulated material needed to be a reasonably stiff mixture. To create such a mixture, Aggregate Base Course (ABC) was mixed with Number 467 stone and coarse concrete sand to create a well graded testing medium with an appropriate level of fines. To maintain a reasonable level of workability due to the maual labor involved, we decided to limit the particle size to less than 2 inches. The testing materials were obtained locally. The ABC and sand were obtained from Godwin Sand and Gravel and the Number 467 stone came from Hamilton Landscaping, both of Raleigh, NC. Figures 10 through 12 show the grain size analyses for the sand, ABC, and No. 467.

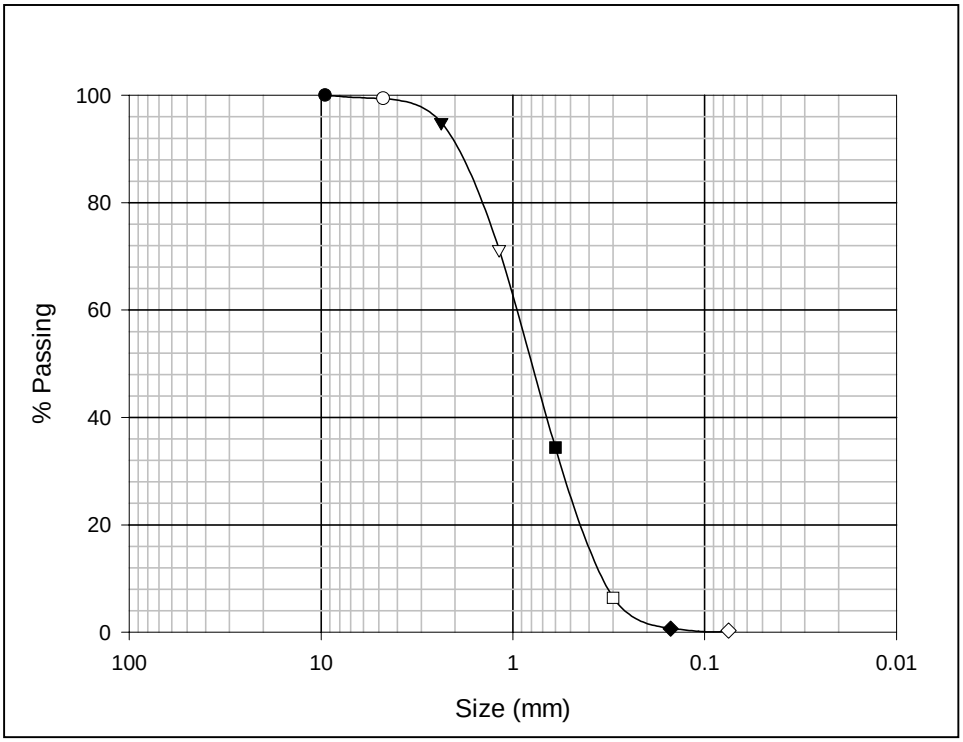

Figure 10 Grain Size Analysis for Coarse Concrete Sand

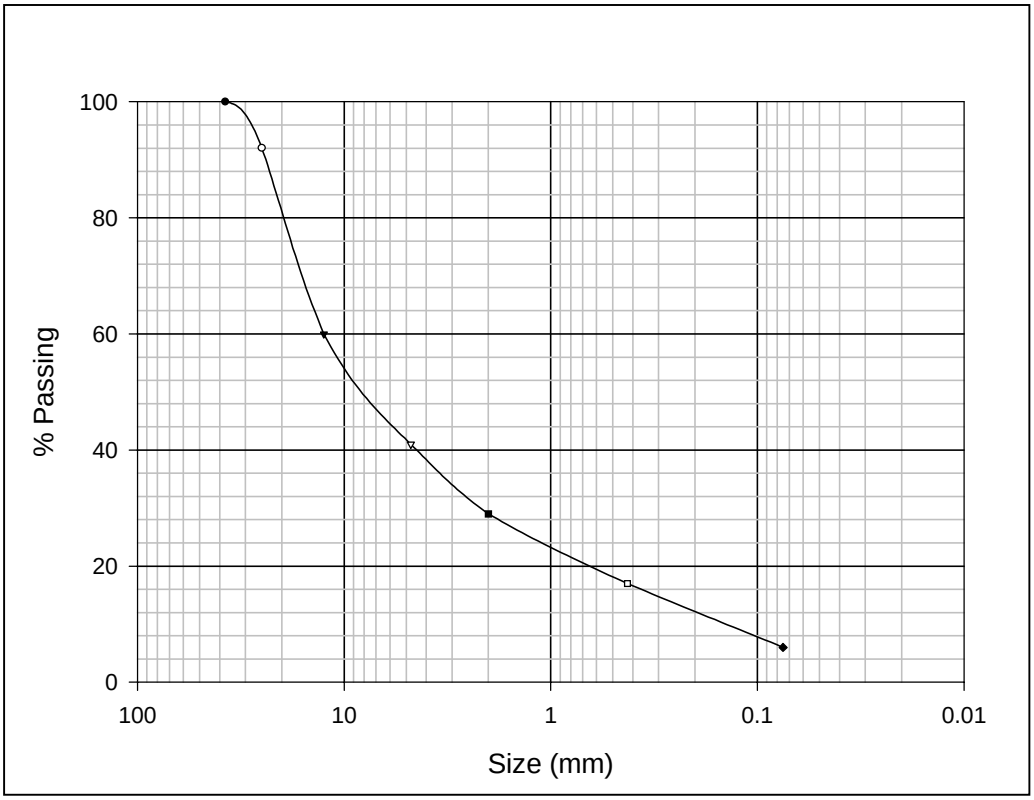

Figure 11 Grain Size Analysis for Aggregate Base Course

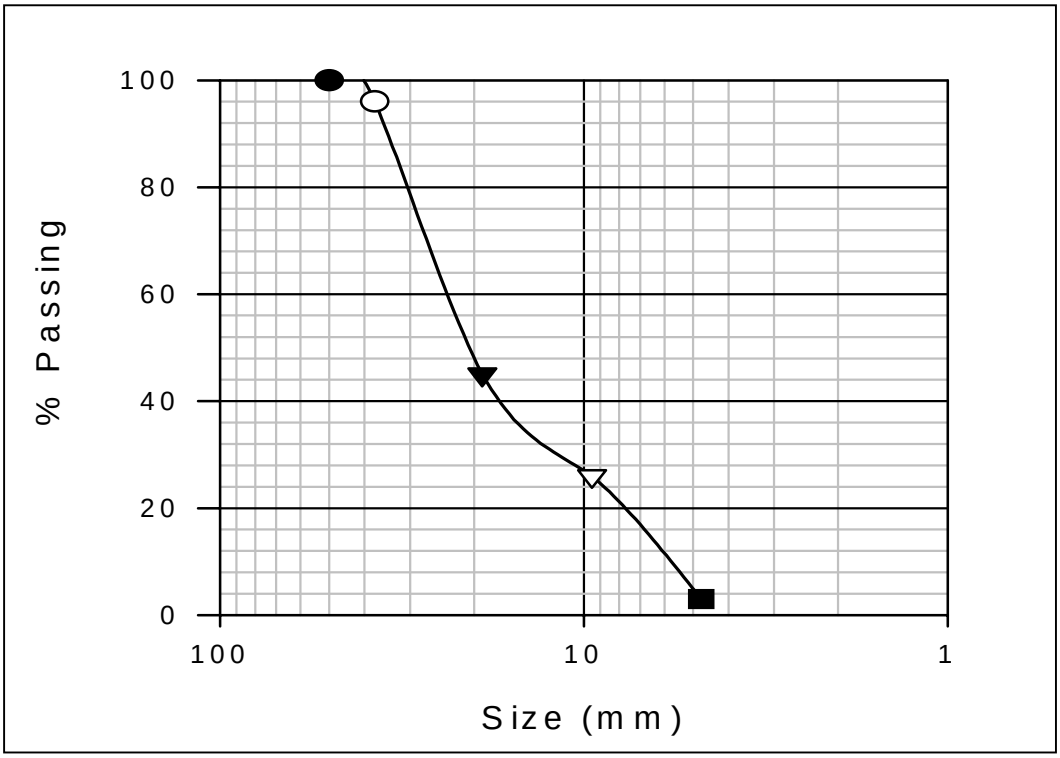

Figure 12 Grain Size Analysis for No. 467 Stone.

The materials were mixed with a Bobcat Loader until the desired consistency was created. The engineering properties of this mixture were evaluated to better understand the behavior of the testing medium. A grain size distrubution of the testing medium is displayed in Figure 13, below.

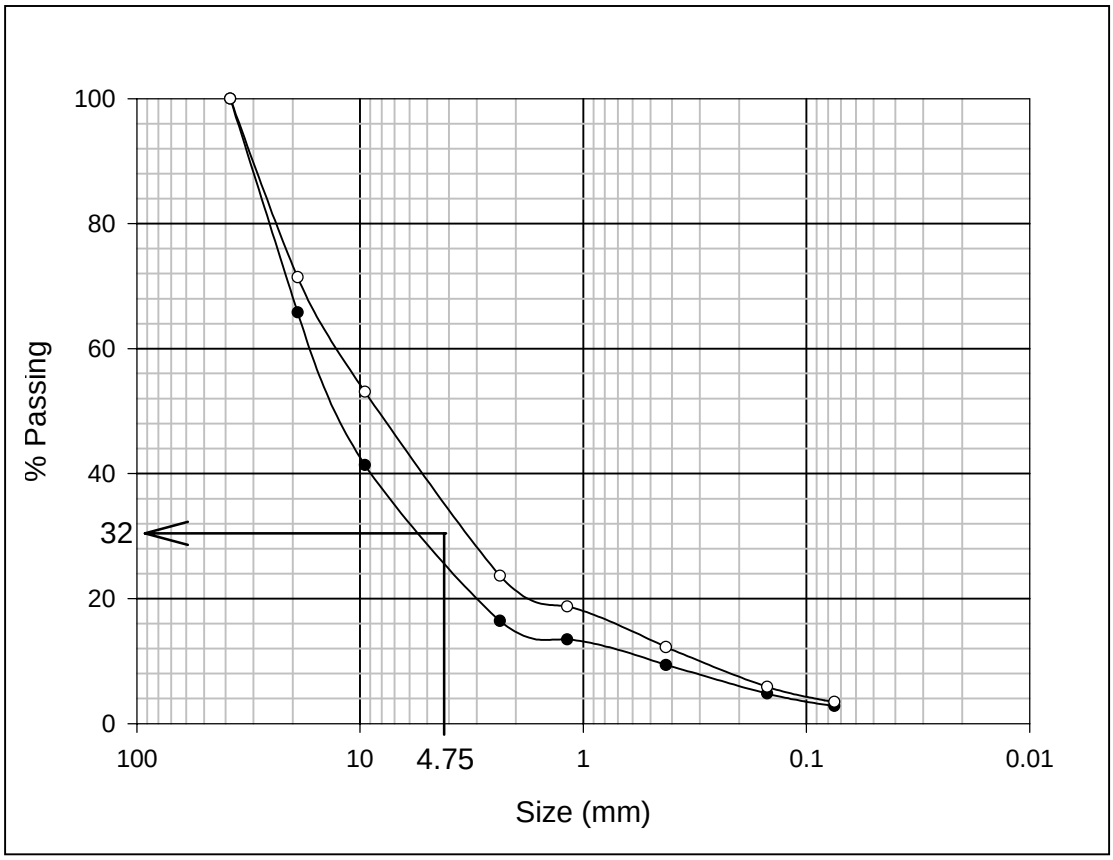

Figure 13 Grain Size Analysis of ABC Mixture

According to the GSA depicted in Figure 13, the soil passing the No. 4 sieve is approximately 32% which is close to the targetted range. From this graph, the coeffiecient of uniformity and coefficient of curvature can be calculated. These values are as follows:

$$c_u = \frac{D_{60}}{D_{10}} = \frac{12}{0.45} = 26$$

$$c_c = \frac{(D_{30})^2}{(D_{60} * D_{10})} = \frac{4^2}{(12 * 0.45)} = 2.96$$

These values indicate the testing medium to be a well graded, clean gravel with less than 4% fines passing No. 200 sieve. Based on these results, the USCS classification of the testing medium is GW, a well graded gravel.

Triaxial Testing

To evaluate the stiffness of the test mix, consolidated drained (CD) triaxial testing was performed. This testing was performed under two different densities to create a range for comparison with the varying densities found in the actual weathered rock masses. The material tested was the ABC mix less any aggregates larger than 0.75 inches. The larger particles were removed due to the size of available testing equipment. A size ratio (length/diameter) of 3-to-1 was desired to prevent gross variation in behavior. The triaxial samples were created using a split mold sampler that was held together tightly with hose clamps. A latex testing membrane, .025 inches thick, was stretched into the mold while attempting to limit wrinkling and folding of the membrane. Then, the ABC mixture was spooned into the mold in three lifts and the lifts were compacted using a modified Proctor Hammer. The compaction method consisted of full height drops (18 inches) and either 6 or 25 drops depending on the desired density. Compaction in this manner yielded unit weights ranging from 115 pcf to 142 pcf. Once the sample was constructed, it was weighed and carefully moved to the triaxial testing cell. A small amount of vacuum was applied to the base and the mold was carefully removed. Once the mold was clear, dimensional measurements were made of the sample. To ensure a leak-proof sample, an additional 0.12-inch membrane was placed over the original

sample. This was done to cover small punctures that may occur during the compaction process. Both the top and bottom of the samples were sealed with three o-rings and the confining stress was applied and allowed to sit for 20-30 minutes to allow any consolidation to occur. The samples were sheared at 0.25 mm/min. This value is approximately 1-2 percent strain per minute based on a desired 15 percent strain failure of a 5.6-inch tall sample. The process was repeated for the different confining stresses and the results in terms of measured deviatoric stress-strain curves are shown in Figures 14 and 15.

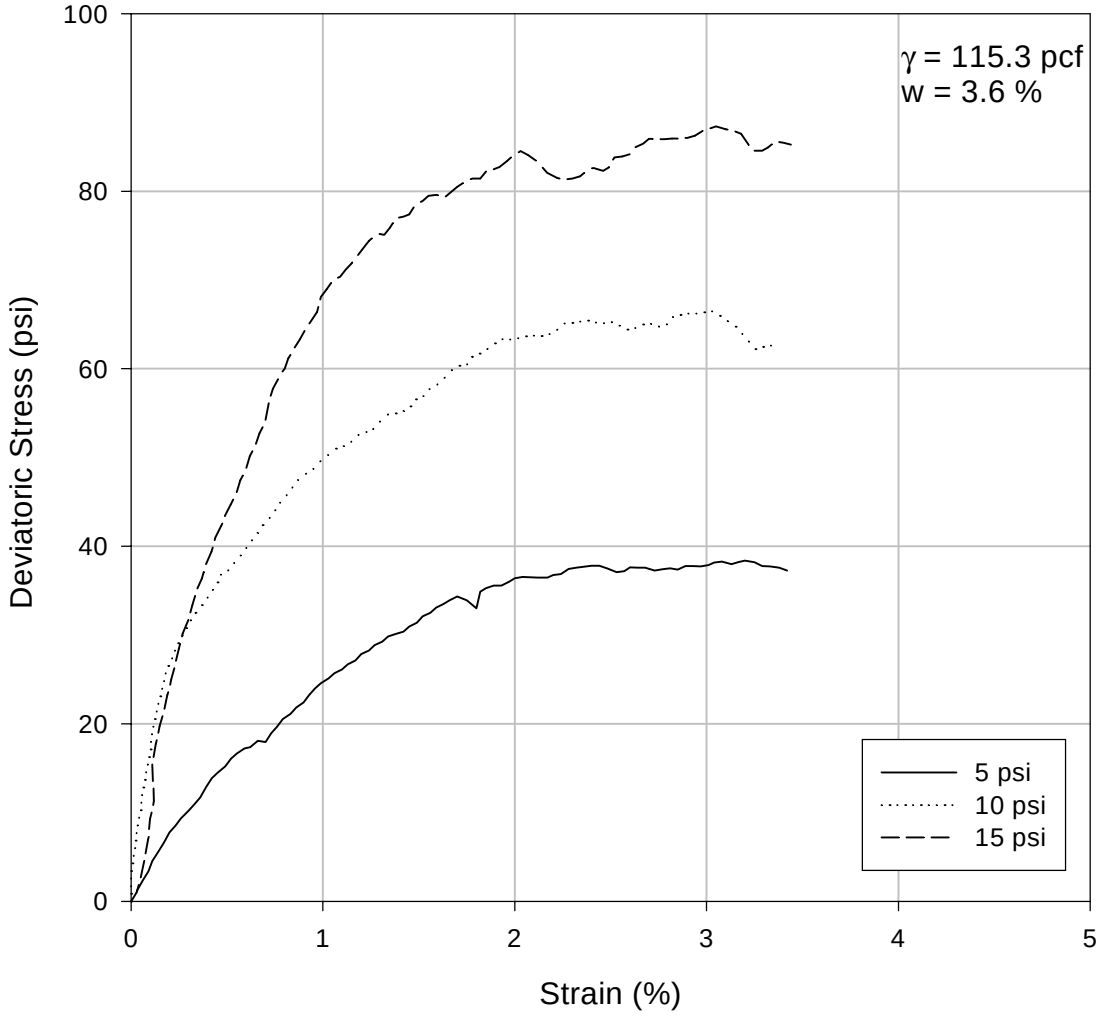

Figure 14 ABC Triaxial Tests (6 blows for density control)

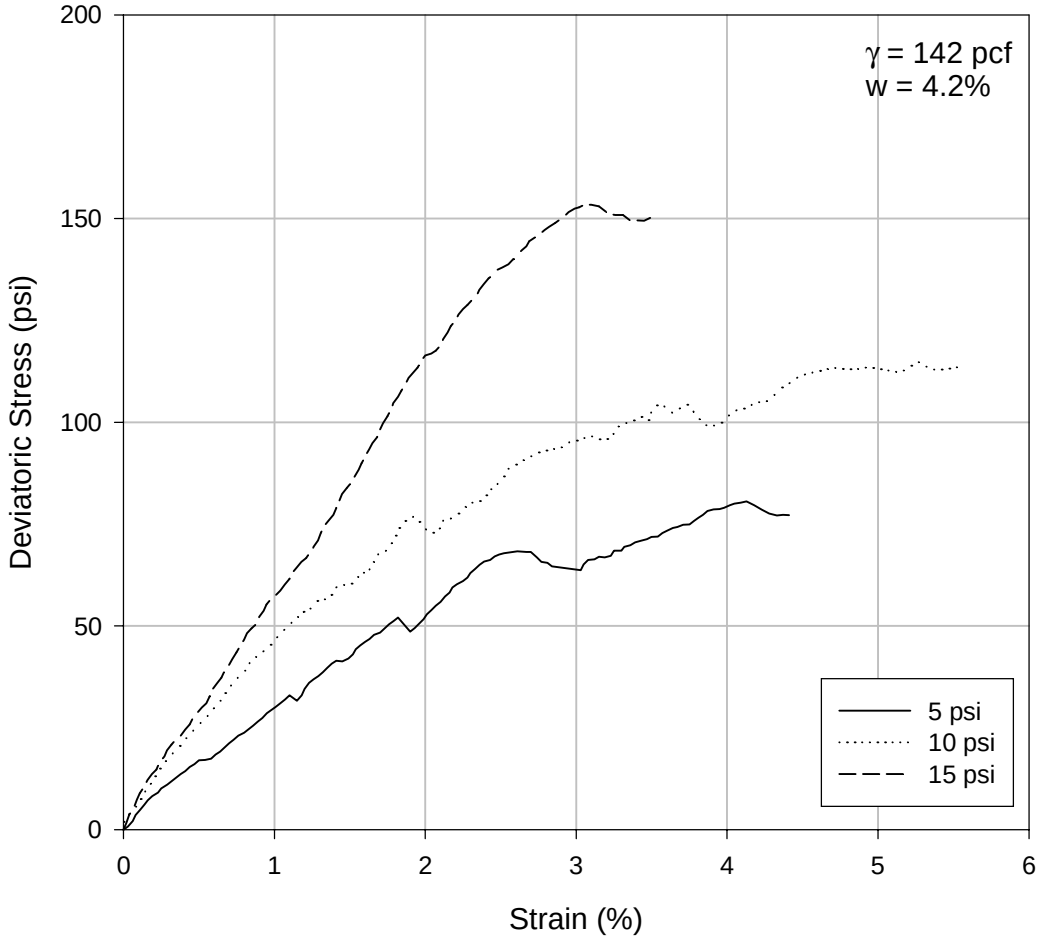

Figure 15 ABC Triaxial Tests (25 blows for density control)

From these plots, the secant modulus of elasticity for the mixture was calculated at a strain level of 2 %. This value was chosen due to the ABC mixture nearing failure at this strain level as seen in Figure 14. The same values were used for consistency to evaluate data in Figure 15. Table 3 shows the secant moduli under various conditions.

Table 3 Modulus of Elasticity of ABC

Confining Pressure (psi)	Modulus of Elasticity (psi)	
	Number of Blows: 6	Number of Blows: 25
5 psi	1800	2750
10 psi	3175	4000
15 psi	4200	5850

Figure 16 depicts the p-q diagrams (stress path) of the samples at failure in the triaxial testing.

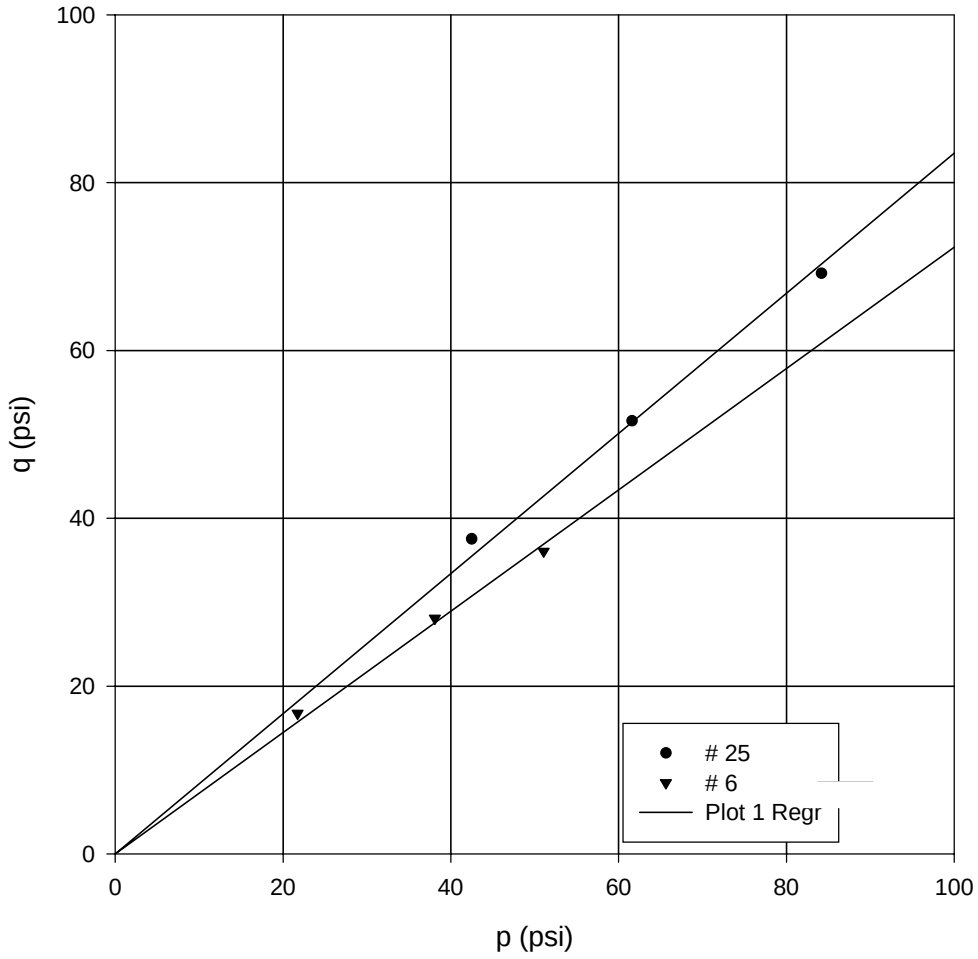

Figure 16 p-q diagram for ABC Mixture.

From these diagrams, the friction angles for the different density ABC mixtures can be calculated using the following equation:

$$\sin\phi = \tan\psi \tag{15}$$

where ϕ = the angle of internal friction, and
ψ = the angle of the K_f line in the p-q diagram.

and the following parameters can be summarized:

Table 4 ABC Properties

Unit Weight (pcf)	# of blows	friction angle, ϕ (degrees)
115	6	46.3
142	25	57.1

3.4 Model Test Piles

The initial set of model piles were constructed of 2.0-inch diameter A36 tubular steel. After the initial testing with coarse concrete sand as the medium, a comparison to a full-scale field test in Nash County revealed that a pile with a higher moment of inertia was required. In this case, the yield strain was reached in the pile's steel material before the desired level of deformation was achieved.

In addition, the field results were analyzed using a pile flexibility coefficient factor introduced by Poulos (1980) to estimate the point of fixity and attempt to simulate it in the laboratory. Under the following assumptions: 1. the P-y curves are linear, 2. the soil is uniform (all P-y curves are the same), 3. the pile is infinitely long, the governing differential equation can be described as follows:

$$EI\frac{d^4y}{dz^4} + Ky = 0 \tag{16}$$

or

$$y = \frac{l_0^4 d^4 y}{4dz^4} \tag{17}$$

with

$$l_0 = \sqrt[4]{\frac{4EI}{K}} \tag{18}$$

This parameter l_0 is called the transfer length. A pile will be considered as infinitely long if:

$$L \geq 3\ l_0$$

The pile is considered rigid if the embedded length L is smaller or equal to the transfer length:

$$L \leq l_0$$

Based on our analysis of the laboratory test results using the 2-inch diameter piles, a fixed condition was reached within a few inches. In order to evaluate the effects of fixity, a larger pile was needed. The second pile diameter was 3.5 inches with a wall thickness of 0.216 inches and a modulus of elasticity = 4.32 x 10^9 lb/ft^2. The moment of inertia (I) = 3.02 in^4.

3.4.1 Pile Properties

The engineering properties of the piles are listed in Table 5. The piles were made from A36 steel with a modulus of elasticity equal to 30×10^6 ksi. The length of the test pile was 4 ft and the diameter used for the results reported herein was 3.5 inches. The moment of inertia (I) for this pile diameter is 3.02 in^4 and EI=9.06x10^7 k-in^2.

Table 5 Properties of Piles

Items	Pile 1 Property Value	Pile 2 Property Value
Modulus of Elasticity (ksi)	30×10^6	30×10^6
Poisson's Ratio (ν)	0.15	0.15
Length of Pile (ft)	4.0	4.0
Diameter of Pile (in)	2.0	3.5

3.4.2 Test Pile Construction

Two identical test piles were constructed for testing in ABC. These piles were constructed of 3.5 in O.D. A36 steel pipe. The wall thickness of this member was 0.216 inches. The instrumentation attachment method for these shafts consisted of drilling 1/8th inch holes every 4 inches. These holes were then reamed to remove sharp burrs from the edges. The strain gages were attached every two inches, beginning four inches from the tip. Once the strain gages were attached, the gage wires were treaded through the openings, thus allowing the instrumentation wire to be protected within the pile member. The gages were then covered with abrasion resistant material and then also covered with metallic tape for further protection.

3.4.3 Model Pile Instrumentation Installation

The purpose of surface preparation is to develop a chemically clean surface with an appropriate roughness, relatively neutral pH, and visible gage lines for installation. The general procedure for the surface preparation is as follows:

1. Solvent degreasing – This removes all surface oils, greases, organics, and soluble residues that occur during manufacture, transportation and installation.
2. Surface Abrading – The surface is abraded to remove loosely bonded materials. In the case of the test pile surfaces, this was accomplished by using varying grades of sandpaper. The grades began with 100 or 200 grit and increased to final grit of 400 to create the desired final surface finish.
3. Gage Layout and Location Lines – Great care was taken to ensure the gages were located along the centerline of the piles and these locations measured.
4. Gage Attachment – Once the locations were identified, the cleaned surface was lightly coated with M-Bond 200 Catalyst to accelerate the bonding process. M-Bond 200 Adhesive was then applied and the gage followed. Care was taken to ensure that the bond did not contain air bubbles. The gage was then covered with Scotch © tape to hold the unit in place until curing was finished.
5. Final Cover – Once curing was completed, the gages were covered with M-Coat to seal the edges. Once this dried, the gages were then covered with abrasion resisting rubber covers.

3.5 Test Chamber Filling Procedure

The test chamber was filled with the ABC mixture using 4-6 inch lifts. These lifts were compacted with a Multiquip MVC-90H. This compactor is a gas operated vibrating plate tamper which can develop a tamping force of 3350 pounds based on a plate size of 20” x 22”(Sunbelt). On alternating layers, the edges were compacted further with a Bosch 11304 Electric Jackhammer equipped with a 12” x 12” steel foot. To determine a target density, a compaction process involving compacting in a circular motion around

the pile locations and parallel to the edges was performed for 3 minutes. The density was then measured with a Troxler Nuclear Gage. The hardened surface was scarified prior to adding additional layers. Another lift was added and the compaction process repeated with the edges being compacted with the jackhammer. Again the density and water content were measured. Once the target density was determined, the compaction process was then repeated for the remaining layers. The properties were "spot checked" to ensure consistency and maintained within +/- 5 pcf (2 % w). When the desired pile tip elevation (18 inches) was reached, the test piles were installed and held plumb using a 2-foot level. The testing medium was then compacted around the piles with the jackhammer. This process continued until the chamber was filled. Once the chamber was filled, the top was leveled and a thin layer of sand applied to ensure an even distribution of the applied stresses; then the loading system was installed.

4.0 INSTRUMENTATION AND DATA ACQUISITION

In order to collect data conveying laterally loaded model pile behavior, a variety of instrumentation is needed. To determine longitudinal strains, electric resistance strain gages from Micromeasurements were used for their applicability. A discussion of the theory behind the use of measured strain to back figure load and deflection follows. In addition to the strain measurement, the displacement behavior was also monitored. The lateral deflections were measured with an electronic dial gage. Rotations at the point of load application were measured with a Schaevitz electronic inclinometer. Another aspect of these tests involves the application of a surface surcharge, where the pressure distribution was monitored with depth. The confining stress increases with depth, around the test piles, was monitored using a series of Geokon pressure cells embedded in the testing medium.

4.1 Instrumentation

Electrical Resistance Strain Gauges, Model CEA-06-250UW-120, were obtained from Micro-Measurements. The CEA family of strain gauges are general use gauges commonly used for stress analysis. They have an applicable thermal range of –100 degrees to +400 degrees Fahrenheit. Each gauge is designed with a ¼" gauge length and overall dimensions of 0.45 inches by 0.18 inches. All gauges used on the test piles had a gage factor of 2.065. The strain in an element is transmitted to the gauge through an adhesive bond. This imposed strain causes gauge elongation or compression of the electrical grid present in the gage. The length changes affect the resistance present in the

grid. The changes in resistance can be measured and converted to units of strain with the given gauge factor.

The gages used in these analyses arrived pre-wired with a 3 conductor strain gauge lead wire. This wiring is suggested by the manufacturer for general purpose environments with a temperature range of –60 degrees to +180 degrees Fahrenheit. The wire was 26 gauge, tinned stranded copper with vinyl coating. .

The strain gauges were attached with a bonding agent, M-Bond 200 Adhesive, also obtained from Micro-Measurements. This general-purpose product is commonly suggested by the manufacturer for environments of –320 degrees to 200 degrees Fahrenheit. M-Bond 200 is an Ethyl Cyanoacrylate based rapid cure adhesive. After setting, this bonding agent has sufficient resistance to moisture and chemical attack. The most significant drawback of this adhesive is the short pot life of 1-2 minutes, thus requiring efficiency in the installation of multiple gauges.

To protect the gages and wiring, the gages were covered with Strain Gauge Weatherproofing, the M-Coat F Kit, from Micro-Measurements. The M-coat F Kit includes an assortment of neoprene rubber sheets, butyl rubber sealant, air-drying nitrile rubber coating, aluminum foil tape and teflon tape. When applied properly, the protective system has an excellent record of protecting strain gauges in field applications such as bridges, tunnels, reinforcing bars, and heavy machinery.

Rotations were measured at the point of load application with a Schaevitz Accustar Electronic Tiltmeter (Schaevitz). This instrument was attached to the shaft with plastic ties. Lateral movements were measured with a Humboldt electronic dial gage with an accuracy of 0.0001 in.

Vertical pressures were measured with Geokon earth pressure cells (EPC). These instruments are designed to measure total pressure in earth fills and embankments. The cells consist of two circular stainless steel plates welded together at their periphery and spaced apart by a narrow cavity filled with antifreeze solution. Changes in pressures are measured by a vibrating wire pressure transducer (Geokon, 8/98).

4.2 Data Acquisition System

All instrumentation was attached to an OPTIM MEGADAC Data Acquisition System. The unit was programmed to take readings every 2 seconds and store the data. These data sets were then downloaded in ASCII format and reduced using commercial software programs.

4.3 Analysis of Laboratory Strain Data

The recorded strain data consists of values of microstrain for a given load at differing depths. Through integration and differentiation, these data can provide load and deflection values as the depth increases. This is based on the assumption of a linearly elastic material, of which steel is as long as the yield stresses are not exceeded. The strain gages are attached to the extreme fibers in the steel, thus 'y', in Figure 17, equals 1.75 inches on average. These strain gages are measuring the longitudinal strains along the tension side of the pile. Assuming the plane sections remain planar in loading, the extreme fiber will lengthen or contract linearly based on location within the member. This elongation is a function of the curvature, ρ, as shown in equation 19, below.

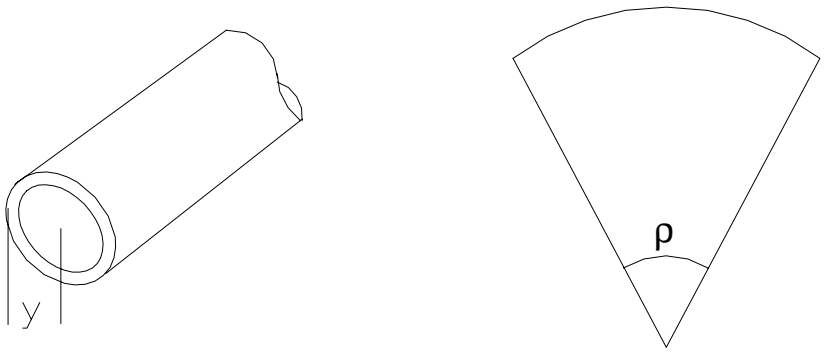

Figure 17 Curvature of Model Pile

$$\varepsilon_x = -\frac{y}{\rho} = -\kappa y \tag{19}$$

where

y = distance to the neutral axis,
ρ = radius of curvature,
κ = curvature of the beam.

The stresses acting normal to the cross section of a beam can be determined from the normal strains, ε_x. Since the steel beam is linearly elastic within our loading range, Hooke's Law for uniaxial stress ($\sigma=E\varepsilon$) can be substituted in to Equation 20 to obtain equation 20 below.

$$\sigma_x = E\varepsilon_x = -\frac{Ey}{\rho} = -E\kappa y \tag{20}$$

where

σ = stress along the x axis,
E = Young's Modulus of the material.

This equation indicates the normal stresses acting along the cross section vary linearly as the distance, y, from the neutral axis changes. In the laboratory piles, the pile cross section is circular and therefore the neutral axis is located along the centerline of the pile.

Given that the moment resultant of the normal stresses is acting over the entire cross section, the resultant can be summarized by equation 21.

$$M_o = -\int \sigma_x y dA \tag{21}$$

Noting that $-M_o$ is equal to the bending moment, M, and substituting for σ_x from equation 21, the bending moment can be expressed as equation 22.

$$M = -\kappa EI \tag{22}$$

where $I = \int y^2 dA$

This equation can be rearranged to the form found in equation 23.

$$\kappa = \frac{1}{\rho} = \frac{M}{EI} \tag{23}$$

This equation is known as the moment-curvature equation and demonstrates that the curvature is directly proportional to the bending moment and inversely proportional to EI, where EI is the flexural rigidity of the beam.

Using the collected microstrain, the distance from the neutral axis to each strain gage (1.75 inches) and equation 20, a value for κ was calculated. Using a Young's modulus of 29,000 ksi and a moment of inertia equal to 3.02 in^4, the moment curvature for a given loading can be calculated. This data was plotted with the moment values on the x-axis and depth from the point of load application on the y-axis as seen in Figure 18.

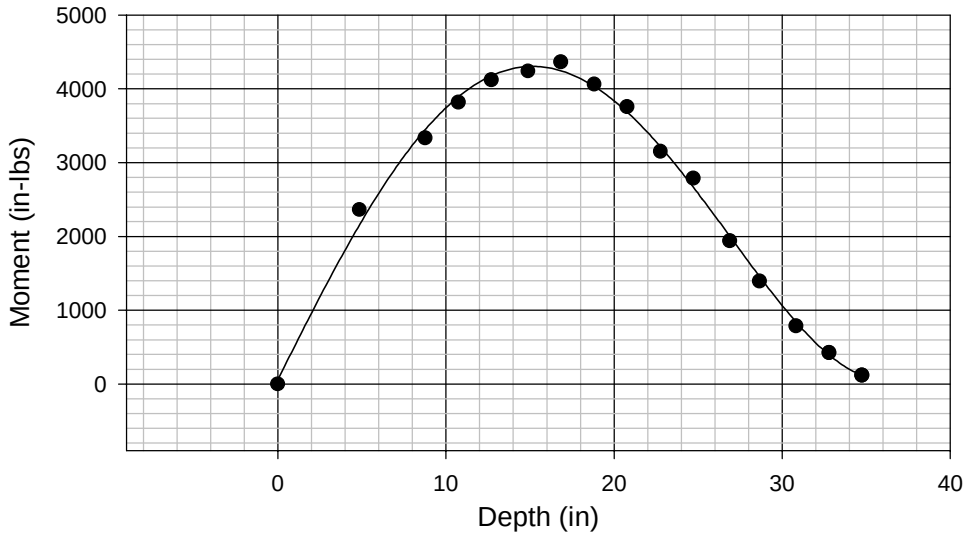

Figure 18 Typical Moment Curvature regression

A fourth order regression line was selected and the corresponding variable values were obtained. This equation is of the following form

$$y = b + b(1)x + b(2)x^2 + b(3)x^3 + b(4)x^4 \qquad (24)$$

where,

b = the coefficient of the regression line,
x = pile segment thickness with the units of inches.

Once equation 24 was obtained, it was differentiated, with respect to x, three times to obtain the load P, in pounds. This equation was also integrated twice to obtain y, in inches. These values were then plotted and thus creating the P-y curve for the pile under a given loading. The process was repeated for all loading increments in each load test.

4.4 Pile Testing Procedure

In general, the horizontal load was applied using a 20-ton Enerpac hydraulic jack controlled with a hand pump. The load was applied in 20 psi increments which equates

to 100 pounds given a loaded area of 5 square inches (the effective area of the jack piston). The load was held until the lateral movement was stabilized and then increased to the next increment. This process was repeated until the maximum strain or soil failure was obtained. The maximum strain was defined as:

$$\varepsilon_{yield} = \frac{\sigma_{yield}}{E} \tag{25}$$

Where σ_y = yield stress or 36000 psi,
E = Young's Modulus, 29000 ksi and,
ε_{yield} = yielding strain.

From this evaluation, the allowable strain was taken as 80 percent of the steel's yield strain or approximately 1000 microstrain. The onset of soil failure was defined as the point when lateral movement was no longer linear.

4.4.1 No Surcharge

A test pile was embedded 34 inches into the compacted ABC mixture. The pile was loaded laterally in approximately 100 pound increments. After each loading, the lateral deflection, top rotation, stress, and strain at each of the gage locations was recorded. Once the lateral movement was stabilized, the next load increment was applied. This process continued until the maximum allowable strains were encountered. Once the test was completed, the chamber was excavated and set up for the next test using the previously defined procedure. Utilizing the moment regression procedure as noted earlier, the deflected shape and corresponding P-y curves were derived for the test results.

4.4.2 With Surcharge

A test pile was embedded 42 inches into the compacted testing medium. The surcharging system was installed and a surcharge of 500 psf was applied and allowed to stabilize. Approximately one hour later, the lateral loading sequence began. As before, the lateral deflection, top rotation, load, and strain were recorded. Again, the test continued until the maximum allowable strains were attained.

4.4.3 Surcharging Procedure

To simulate depth in the laboratory model, a surcharge was applied to the top of the testing medium. The surcharge was applied using two 1" thick steel plates topped with a W6x13 steel beam to distribute the surcharge evenly. The dimensions of the two loaded plates are 24 inches x 66 inches. The actual loading was applied with two 30-ton Enerpac hydraulic jacks. These jacks were loaded between a 200 kip reaction beam and the W6x13 members. To measure the applied force, a 50,000 pound load cell was placed between each jack and reaction beam. This load was measured using a P-3500 Vishay box. The surcharging configuration is shown in Figures 19 and 20.

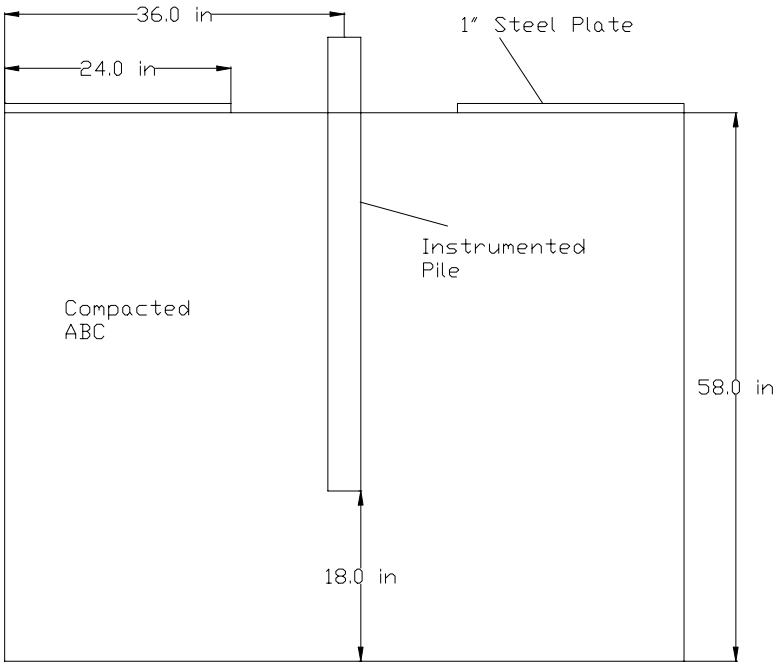

Figure 19 Profile View of the Surcharge system

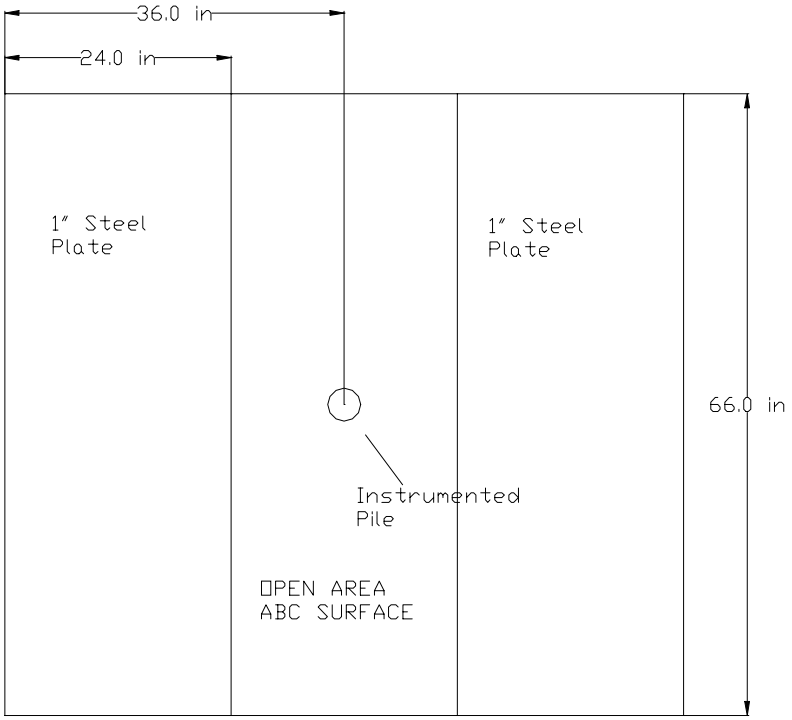

Figure 20 Plan View of the Surcharge system

To determine the stress distribution along the pile length, a series of four Geokon Earth Pressure Cells (EPC) were installed as shown in Figure 21. Only one EPC is depicted, however the remaining three EPCs are located directly beneath the depicted image. The cells were located at the following depths: 7.1, 19.3, 23.5, and 32.3 inches, measured from the ground surface.

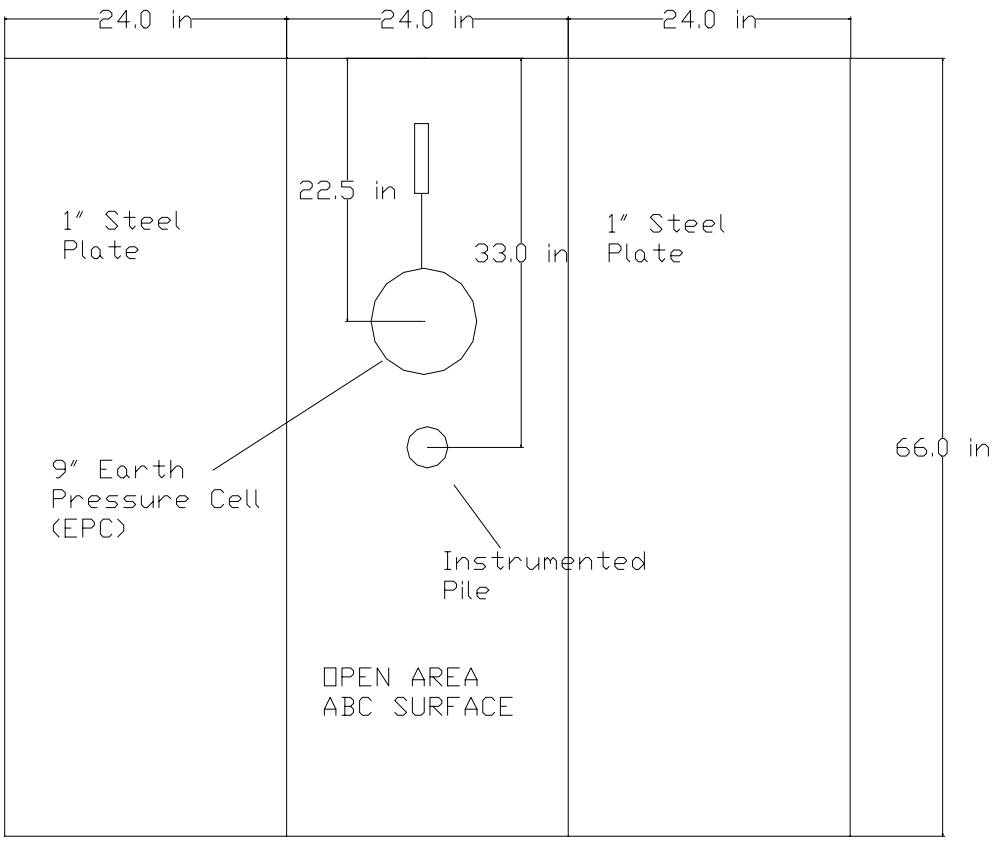

Figure 21 Geokon EPC layout

Once the load was applied, the stress distribution was monitored adjacent to the pile. Figure 22 shows the stress increase with depth as measured from the pressure cells. (please recall that the surface surcharge was applied to the plates, and the pile was located

between the two plates' gap of 24 inches). Assuming a "straight line" stress distribution between the pressure cells, the vertical stress adjacent to the pile increases from approximately 100 psf at the surface to 450 psf at a depth of 2 ft. The measured stresses then reduce to 400 psf at a depth of 2.75 ft. This reduction was due to inadequately compacted ABC at this depth (only around the EPC). The main concern in this case was not to obtain a specific distribution of stresses but to know the magnitude of stresses being applied. Such knowledge is obtained from the stress cell readings. To evaluate the validity of the "straight line" approach, an analysis using a Bousinesq approximation was performed. The results of this analysis is depicted in Figure 22 and demonstrates the "straight line" estimation is valid for depths less than 20 inches, but over estimates the remaining depths. For analyses requiring the stress increase values, the Bousinesq approximations will be used due to the greater depth estimated.

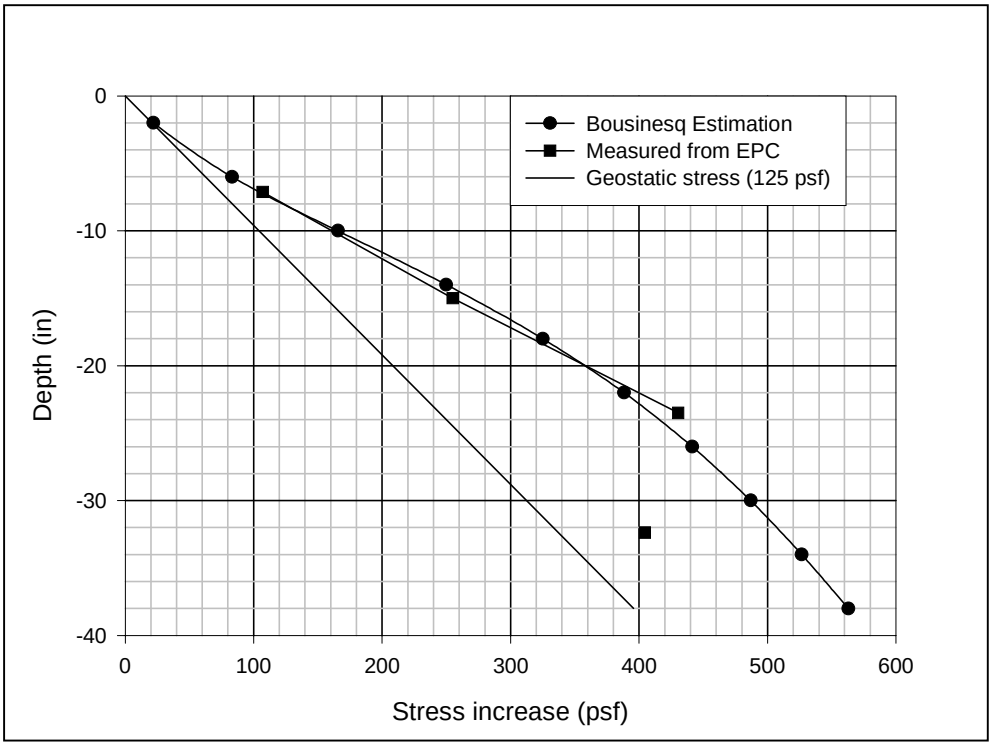

Figure 22 Stress Distribution

5.0 MEASURED P-Y CURVES

The instrumented model piles were used to measure strain data and back figure P-y curves at different depths within the ABC testing medium. This was accomplished through the instrumentation previously discussed. The results are presented in the following sections.

5.1 Pile Testing Results

The measured P-y curves in the testing program are presented in Figures 23 to 27, and indicate a general trend where P-y curves become steeper in slope as the depth increases. The trend line that has been fitted through the actual points is based a hyperbolic function proposed by Konder (1963). This function is based on a transformation of the vertical axis. By transforming this axis, a function of the form is created:

$$y = \frac{x}{a + bx}; \tag{26}$$

where $a = 1/k_h$, or the initial tangent modulus and,
$b = 1/p_{ult}$

For a soil mass to be accurately described by a hyperbolic function, the data points should align into a positive slope. Figures 23 and 24 show the P-y data and the transformed points.

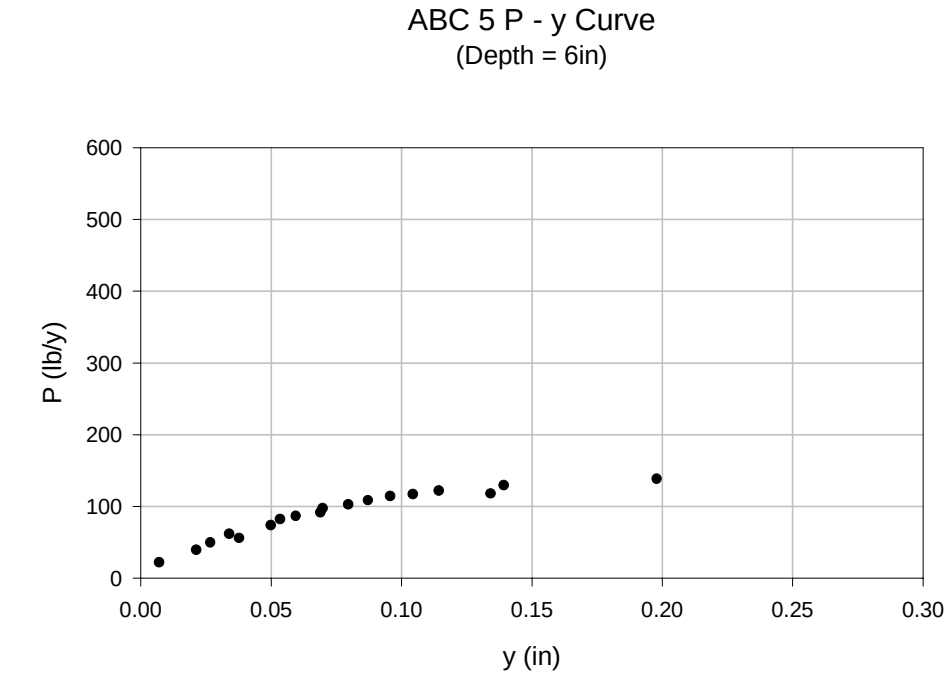

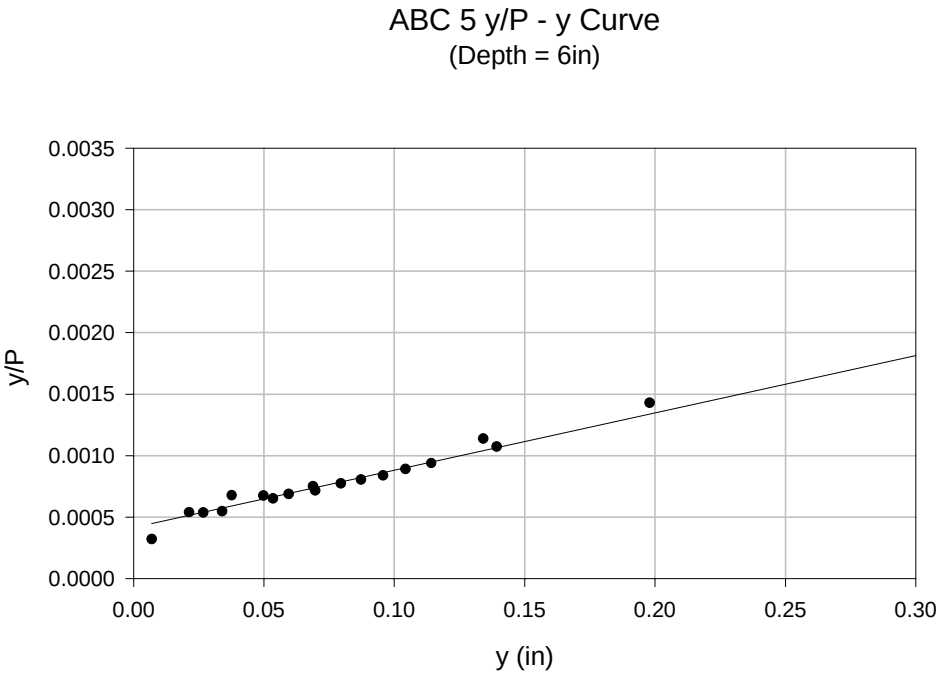

Figure 23 No Surcharge P-y and Hyperbolic Transformation

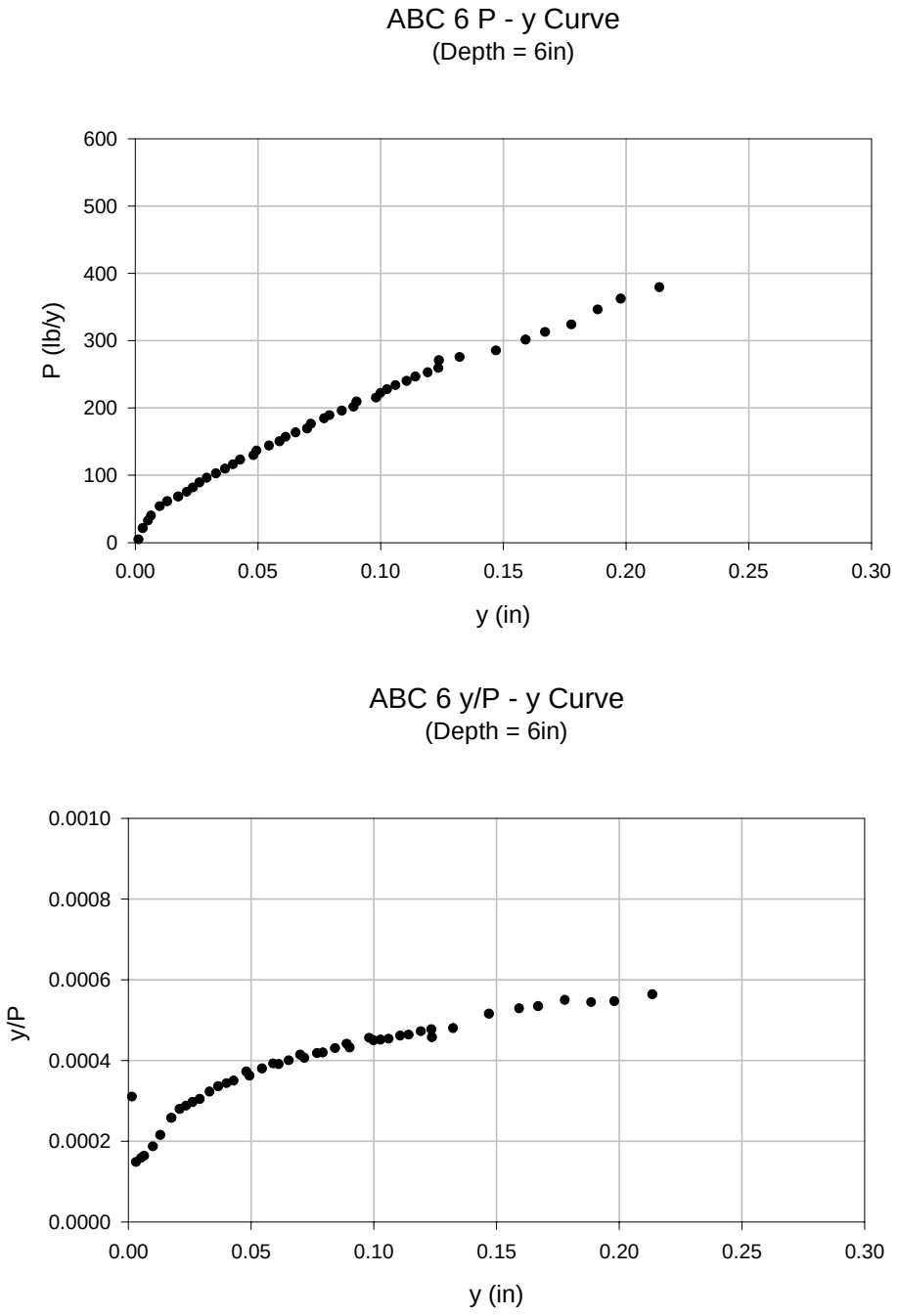

Figure 24 Surcharged P-y Curves and Hyperbolic Transformation

Figure 23 indicates the tests with no surcharge can be appropriately modeled using a hyperbolic function, however the surcharged indicates a significant variation with the initial data points, Figure 24. As the deflection increases, the surcharged data develops

the required alignment. The presence of this alignment will be later used to estimate the P_{ult} for the various depths. This curve fitting procedure was repeated for the measured data with depth down to the point of rotation in the model pile. The data at the depth corresponding to the point of rotation appear as a very tight cluster and the hyperbolic regression equations generate unreasonable results. For these segments, a linear interpolation was made from the last reasonable value to estimate b at the model pile tip (as specified by equation 26).

To determine the value of k_{ho}, an averaging procedure based on the first 4 load increments was performed. The general procedure involved taking the amount of horizontal movement (y) and the required force (P) in one-inch increments for the length of the embedded pile. These values were averaged over the specified load increments. This process obtained a more consistent k_h value. These values were then divided by the diameter of the pile to determine the k_{ho} value.

Figure 25 shows results from the first successful test. The ABC material in this test was prepared with an average density of 105 pcf and moisture content of 4.5 percent. Figure 24 presents results from the surcharged test with an average density of 125 pcf and a moisture content of 5.3 percent. The solid line shown in these graphs represents the hyperbolic curve fitting function as developed in SigmaPlot. The a parameter from the averaging process previously described and the b parameter from the curve fitting constant as provided by the SigmaPlot program are tabulated in Table 6 for both tests. All values presented in the table are based on the inverse, 1/a or 1/b, of the SigmaPlot value or Average Value.

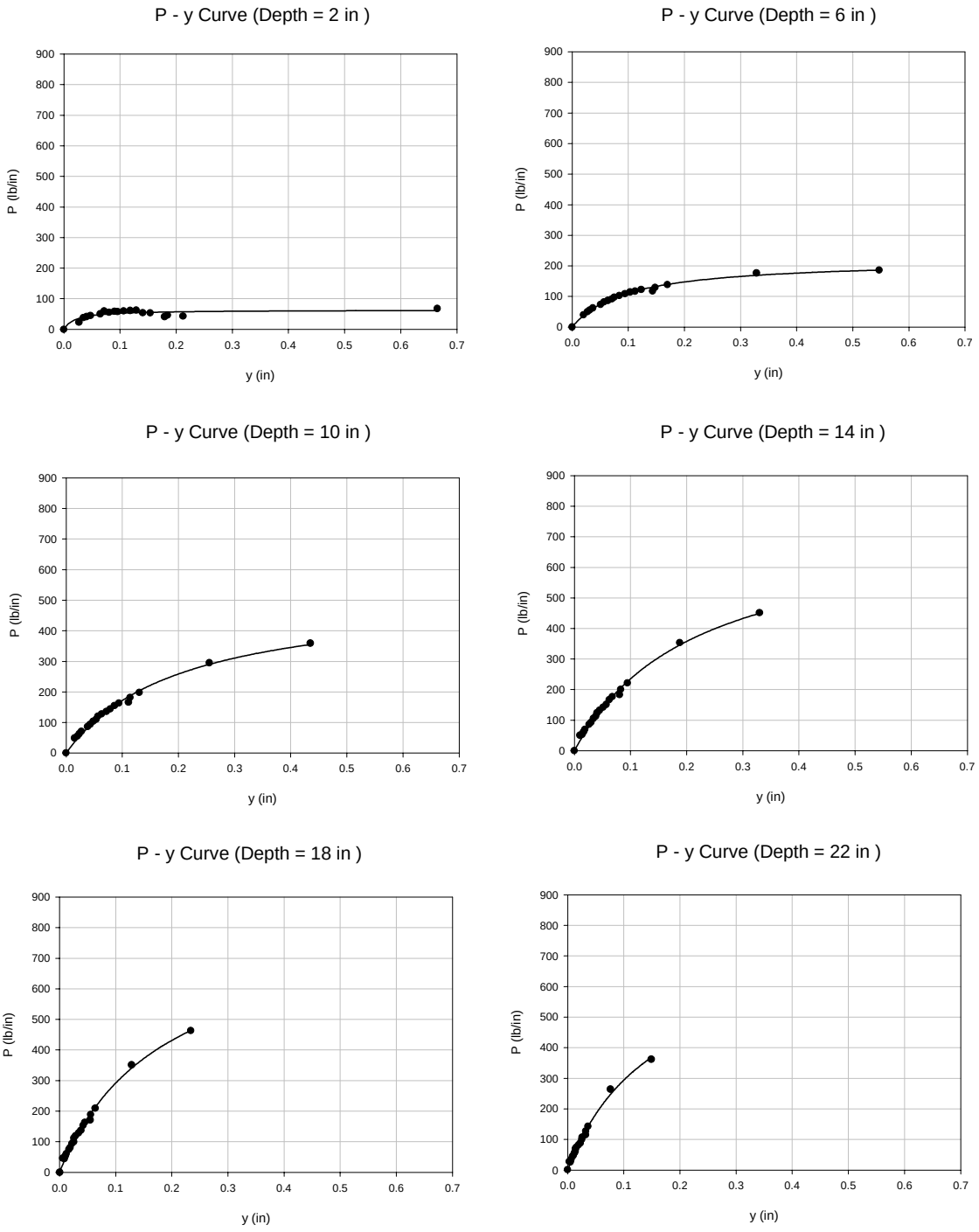

Figure 25 P-y curves for lateral load test with no surcharge.

The evaluated P-y curves shown in Figures 25 and 26 indicated an increase in lateral stiffness with depth as well as increase in the lateral resistance. At the shallower depth, a $P_{ult\ was}$ defined at a deformation level of approximately 0.3 inches. This is equivalent to

approximately 10% of the test pile diameter. After approximately 1 ft of pile depth, it was harder to obtain such a level of deformation and only the initial slope of the P-y curves was evaluated.

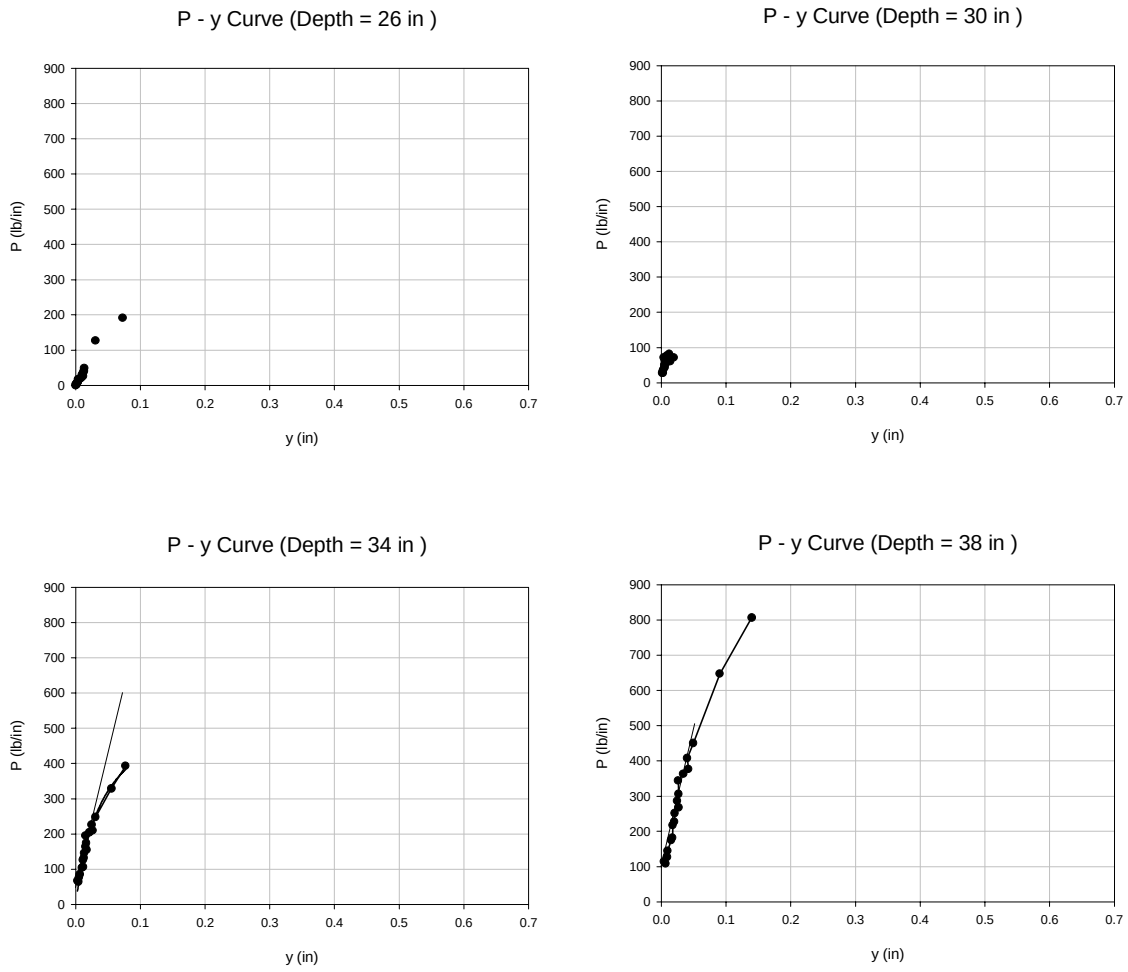

Figure 26 P-y curves for lateral load test with no surcharge (continued).

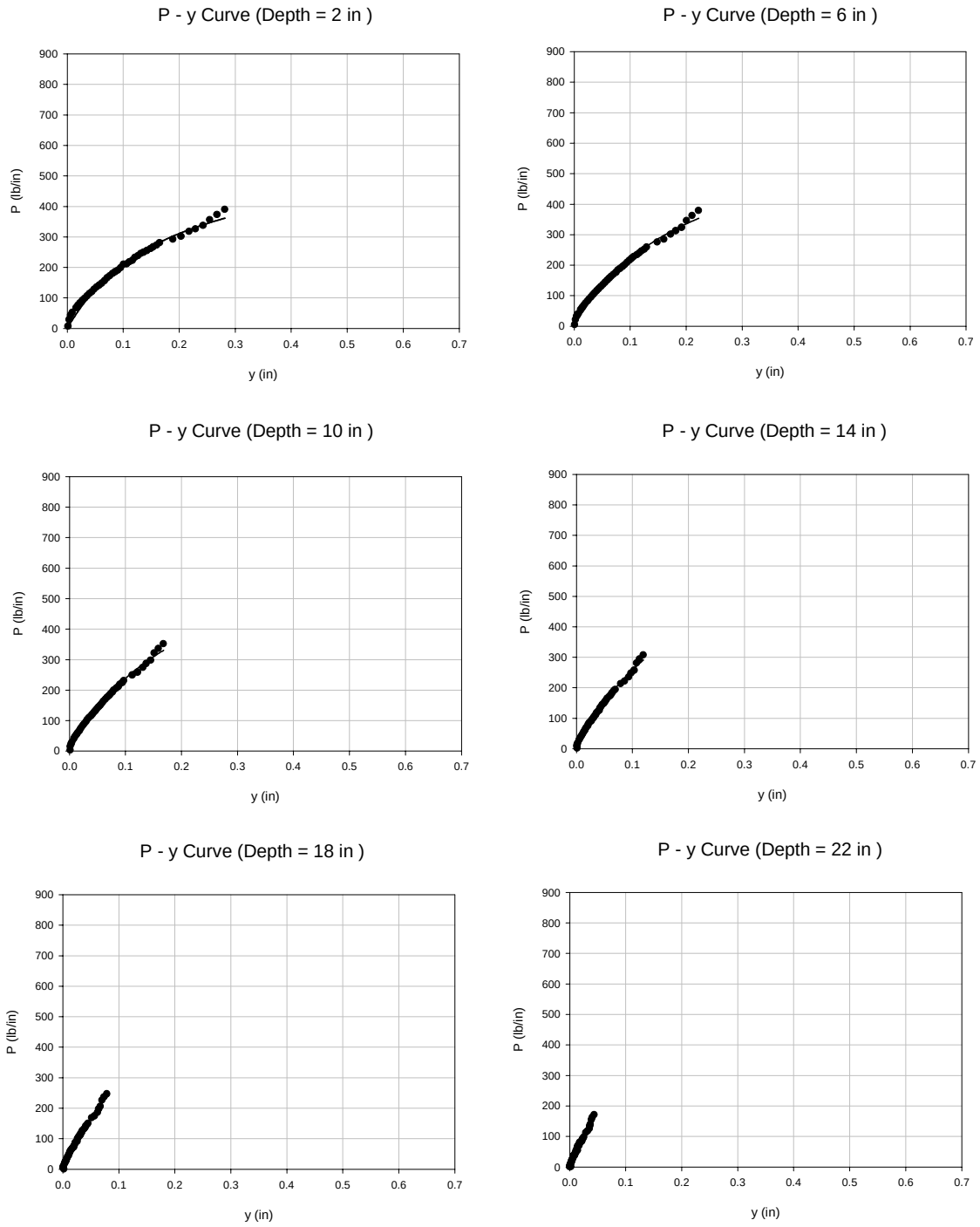

Figure 27 P-y curves for lateral load test with a 500 psf surcharge.

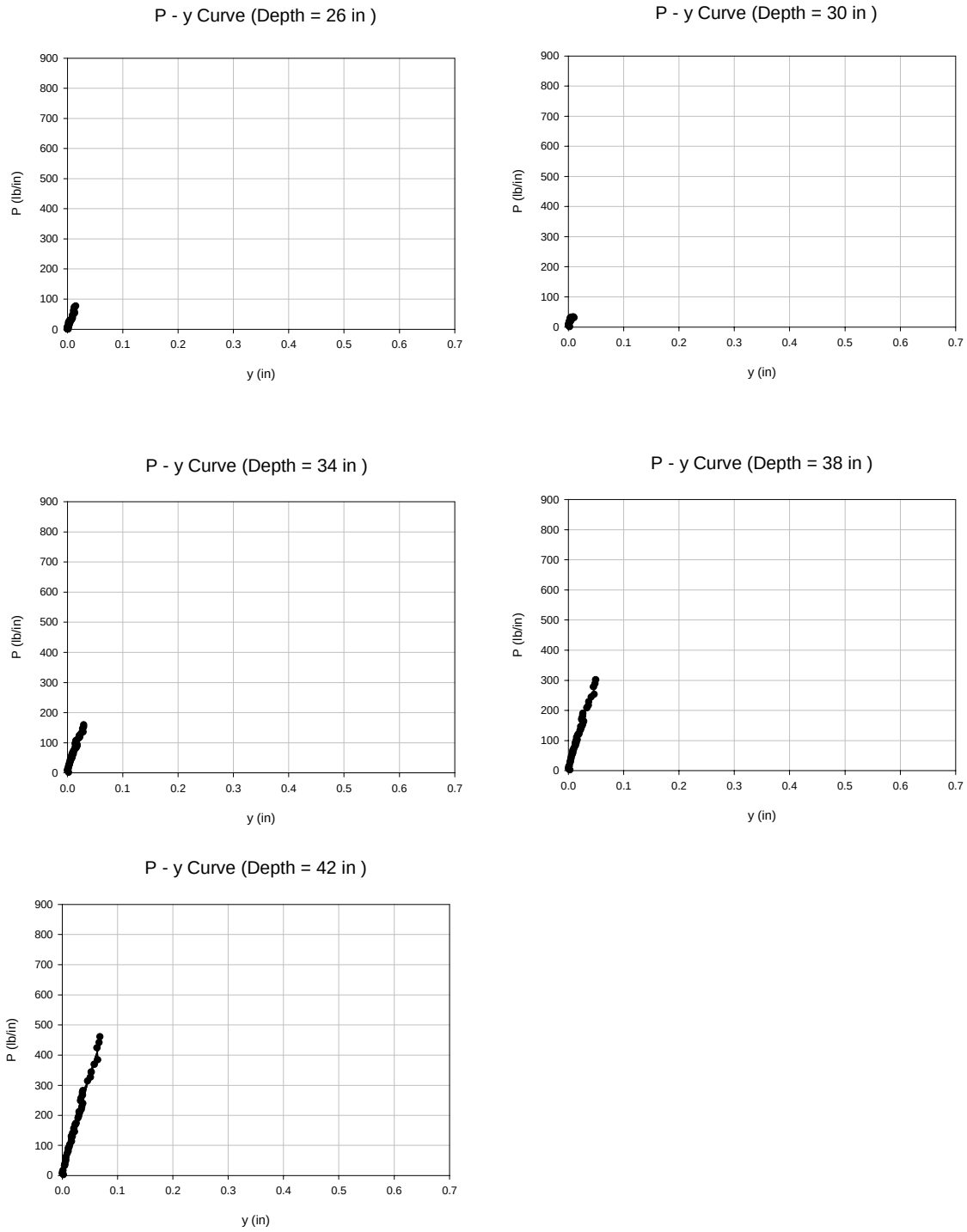

Figure 28 P-y curves for lateral load test with a 500 psf surcharge. (continued)

The P-y results from the test with surcharge shows a trend similar to data shown in Figures 25 and 26. In the case of surcharged test, the load-induced deformation was

not large enough to achieve P_{ult} value. However, the initial stiffness of the P-y curve corresponded well with the confining stress whereby higher lateral stiffness values are evaluated at the depth corresponding to high confining stress.

5.2 P-y curve Parameters

The a parameter determined by the averaging method described previously and the b parameter back figured from the hyperbolic curve fitting are further manipulated in Table 6. Utilizing the hyperbolic function that was curve fitted onto the P-y curves, P_{ult} was predicted by taking the inverse of the 'b' parameter as suggested by Konder et al (1963). The modulus of subgrade reaction, k_{ho}, was the evaluated as an average of the initial loading increments, in the linear range, for each depth. The values for k_{ho} ($lb/in^2/in$) and P_{ult} (lb/in) respectively, are presented in Table 6. However, a gross margin of error may be expected for estimating P_{ult} data from few points that represent the initial part of the P-y curve. This is the case for the test data at depth below 14 inches for pile loaded under surface surcharge of 500 psf and for this case, P_{ult} was not estimated from the data.

Utilizing these parameters, P-y curves containing ultimate P values were determined and input into BMCOL76 to compare measured deflections with predicted values. As shown in Figure 29, the measured and predicted results are relatively close thus indicating these P-y curves are reasonable representation of the behavior of the tested gravelly soil.

Table 6 Summary of a and b parameters

Depth	$k_{ho\ (lb/in^2/in)}$		$P_{ult\ (lb/in)}$	
	ABC 5	ABC 6	ABC 5	ABC 6
-2	255	863	63	600
-6	297	956	220	687
-10	353	1081	520	763
-14	431	1246	745	817
-18	552	1469	826	840
-22	708	1735	**	896
-26	1578	**	**	**
-30	**	**	**	**
-34	**	**	**	**
-38	**	**	1304	**
-42	**	**		1964

** These points were removed from the evaluation due to the lack of data points in the nonlinear portion of the P-y curve

In general, a softer response was consistently predicted using BMCOL76. However it is felt that this difference could be minimized if additional P-y curves could be input into the BMCOL76 program. BMCOL76 allows the user to input up to 10 P-y curves thus introducing some limitations to its use.

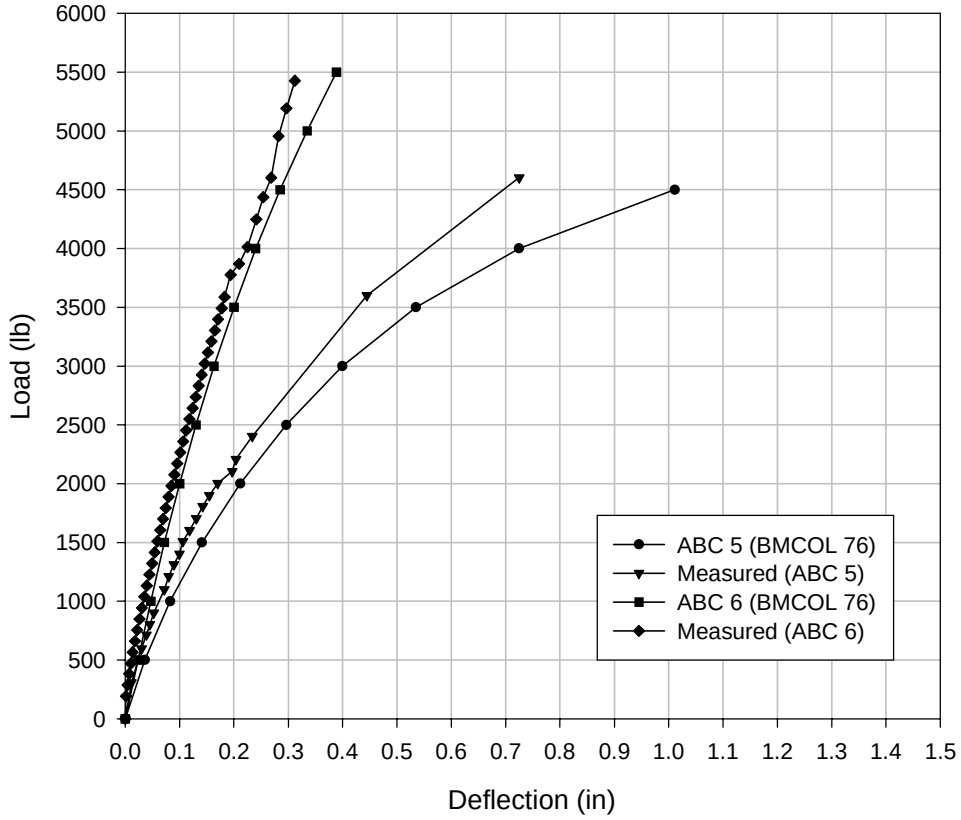

Figure 29 Comparison of Measured and Calculated Pile Top Deflections

5.3 P-y Properties with Depth

Evaluating the values presented for k_{ho} as a function of depth gives an indication of the effects of surcharging. The coefficient of subgrade modulus is shown in Figure 30, for the test sequence.

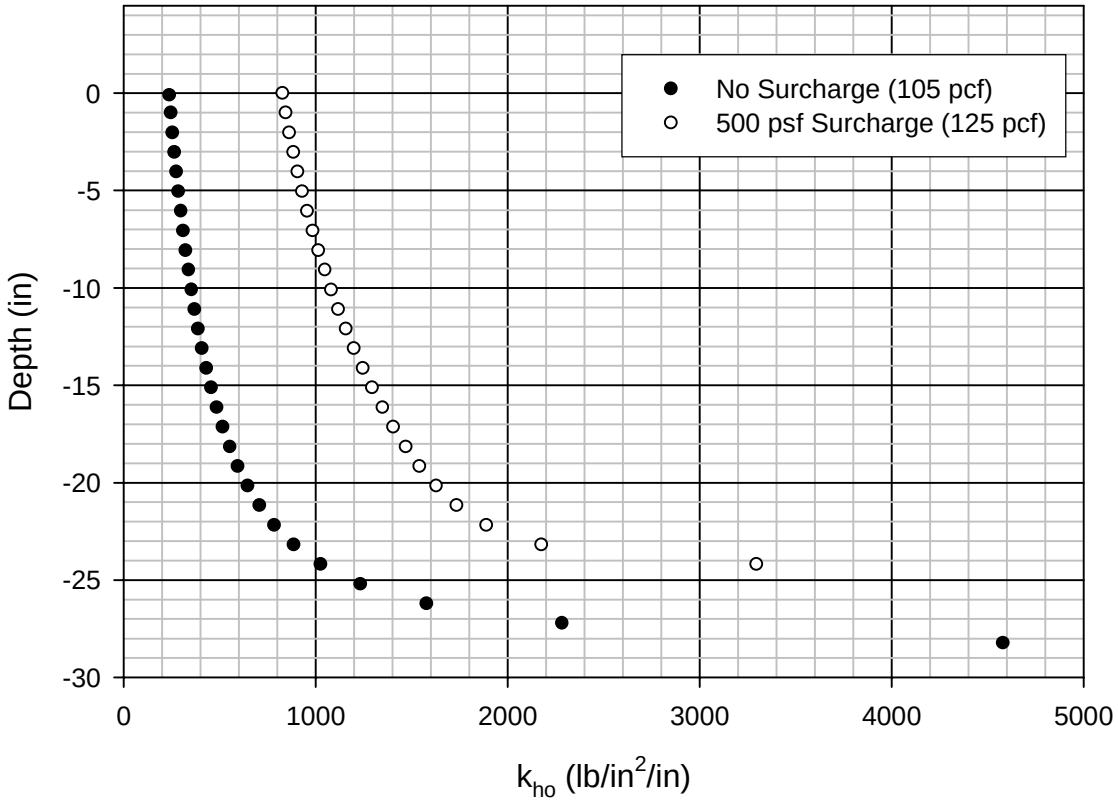

Figure 30 Depth vs k_{hh} – ABC 5 and ABC 6

Combining both figures on one graph shows the effect of the increased confining stress. The data indicates that the modulus of subgrade reaction (k_{ho}) is not a constant value but increases linearly, with depth, to a point and in both cases begins to develop an exponential decay curve. This "decay curvature" likely begins at or near the point of rotation for each pile. The point of rotation is higher in the surcharged test due to the increased density of the testing medium and the application of a surcharge. Since the surcharge was not applied at the edges of the piles, we know the stress increase at this point is equal to zero, thus the difference in k_{ho} is a material property, i.e. a higher density material. If we adjust the curve by subtracting the difference between the two curves, the

increase in k_{ho} due to the application of the surcharge can be seen more clearly. This adjustment is shown in Figure 31.

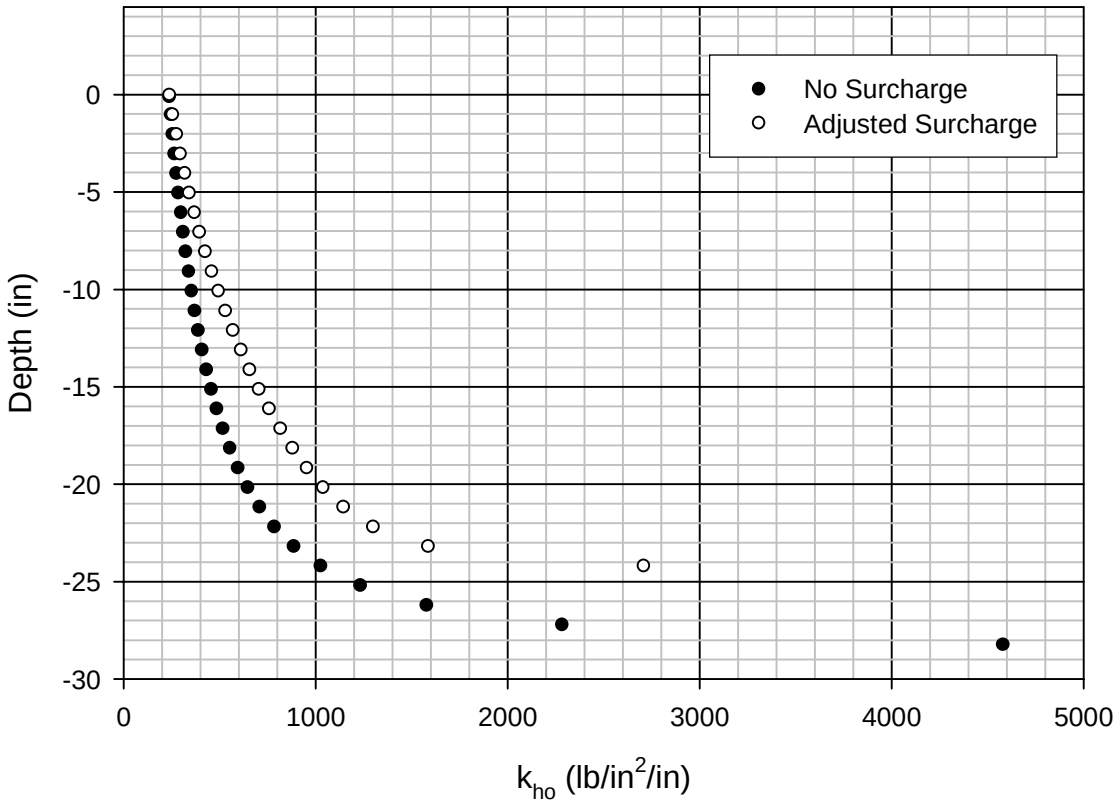

Figure 31 Surcharge Adjusted k_{ho} curves

The results of these test indicate that the value of the subgrade modulus, k_h, is in fact not a constant as assumed by Terzaghi (1955) but follows the trends suggested by Prakash (1962) when he demonstrated these assumptions on a model scale in sands. However, Prakash (1962) indicated the actual variation of the subgrade modulus, k_h, with depth is not fully linear but takes on an exponential decay shape, as indictated in Figure 32, thus indicating an increasing subgrade modulus coefficient value, k_{ho}.

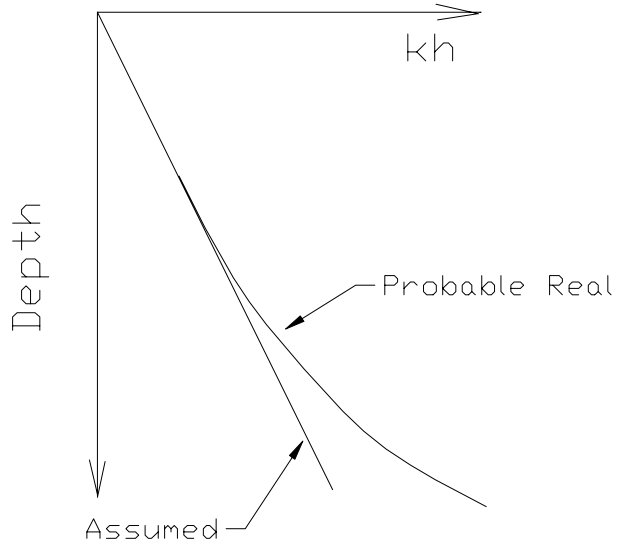

Figure 32 Variation of Subgrade Modulus with Depth (Prakash, 1962)

The application of a surcharge appears to stiffen the testing medium thus causing the k_{ho} response to increase more rapidly for the same depths.

The relationship between depth and P_{ult} can be evaluated by graphically presenting the data in Table 6. Recall P_{ult} was determined from the axes transformation process developed by Konder (1963). Figure 33 depicts the distribution of P_{ult} with depth comparisons for the laboratory tests.

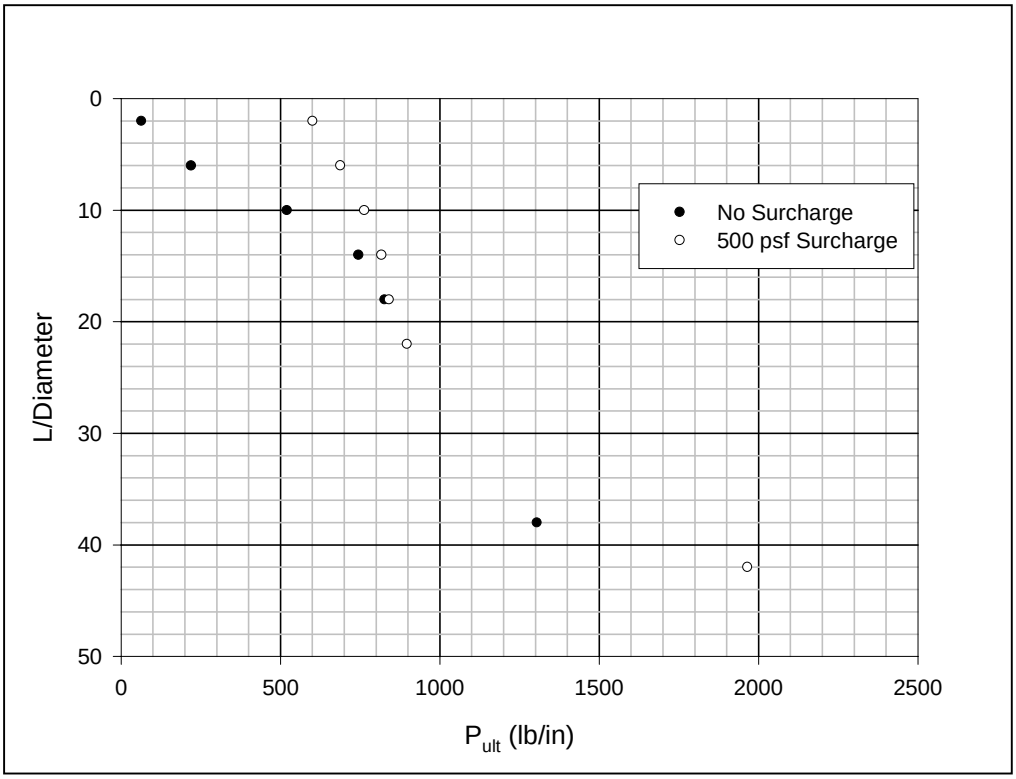

Figure 33 Depth vs Pult – ABC Tests (500 psf surcharge and No Surcharge)

As shown in Figure 33, the test with no surcharge indicates a P_{ult} of approximately zero at the ground surface. Analyzing the results indicates the application of increased confining stresses does in fact increase the ultimate strength of the material. However as discussed previously, after a depth of approximately 14 inches, the ability to predict P_{ult} becomes questionable due the limited number of data points. Evaluation of P_{ult} led to a relationship based on the analysis of the Hoek-Brown failure criterion for rock masses (1998). Based on this criterion, the generalized failure criterion for jointed rock masses is defined by:

$$\sigma_1^{/} = \sigma_3^{/} + \sigma_{ci}\left(m_b \frac{\sigma_3^{/}}{\sigma_{ci}} + s\right)^a$$

where $\sigma_1^{'}$ and $\sigma_3^{'}$ are the maximum and minimum effective stresses at failure,
m_b is the Hoek-Brown constant for the rock mass,
s and a are constants which depend on the rock mass, and
σ_{ci} is the uniaxial compressive strength of the intact rock pieces.

The values of m_b, s and a are based on the value of the Geological Strength Index (GSI) chosen as defined in Figure 34 and are calculated using the relationships in the following table.

Table 7 Relations between m_b, s, and a and GSI [Hoek et al (1995)]

Parameter	Quality of Rock Mass (GSI)	
	Good to reasonable (>25)	Very Poor (<25)
m_b	exp((GSI-100)28)*m_i	exp((GSI-100)28)*m_i
s	exp((GSI-100)9)	0
a	0.5	0.65-(GSI/200)

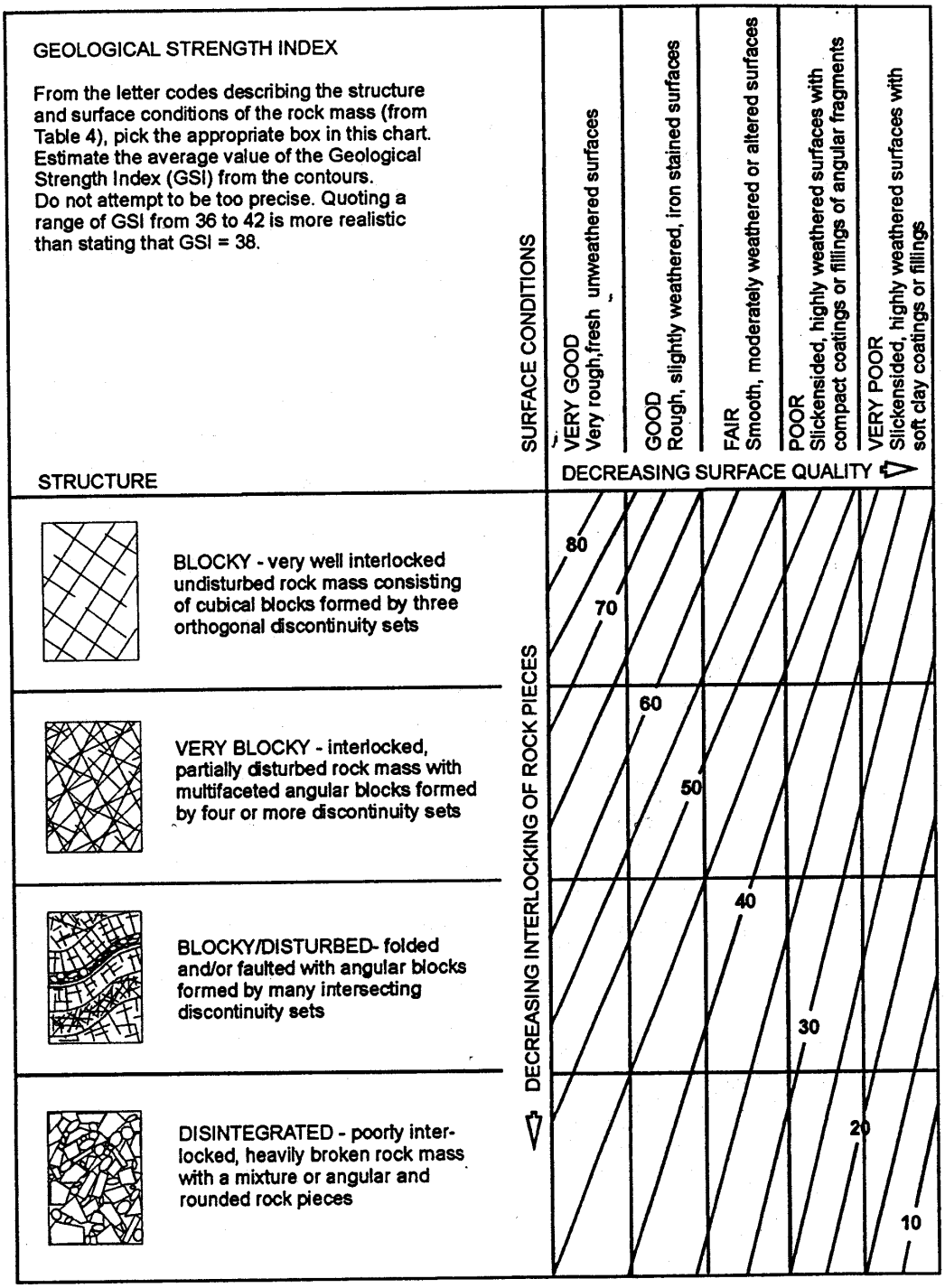

Figure 34 Geological Strength Index (GSI) based on geological descriptions

This criterion was used by Zhang et al. (2000) to determine the normal limit stress p_L and subsequently P_{ult}. Briaud and Smith (1983) and Carter and Kulhawy (1992) have presented the following relationship to estimate P_{ult}:

$$p_{ult} = (p_L + \tau_{max})B$$

where p_L the normal limit stress ,and
$\tau_{max} = 0.20(\sigma_c)^{0.5}$ (Mpa) for a smooth rock socket (Zhang 1999).

Utilizing these relationships, P_{ult} for the laboratory testing was calculated and compared to the values predicted by the hyperbolic modeling technique suggested by Konder (1962). The parameters in Table 8 were used in the estimation calculations. The P_{ult} values for the non-surcharged test and estimated P_{ult} values are shown in Figure 35.

Table 8 Parameters for Estimation of P_{ult}

Property	Value
GSI	10
m_i	10
s	0
a	.55
σ_c	σ'*tan (52 degrees)

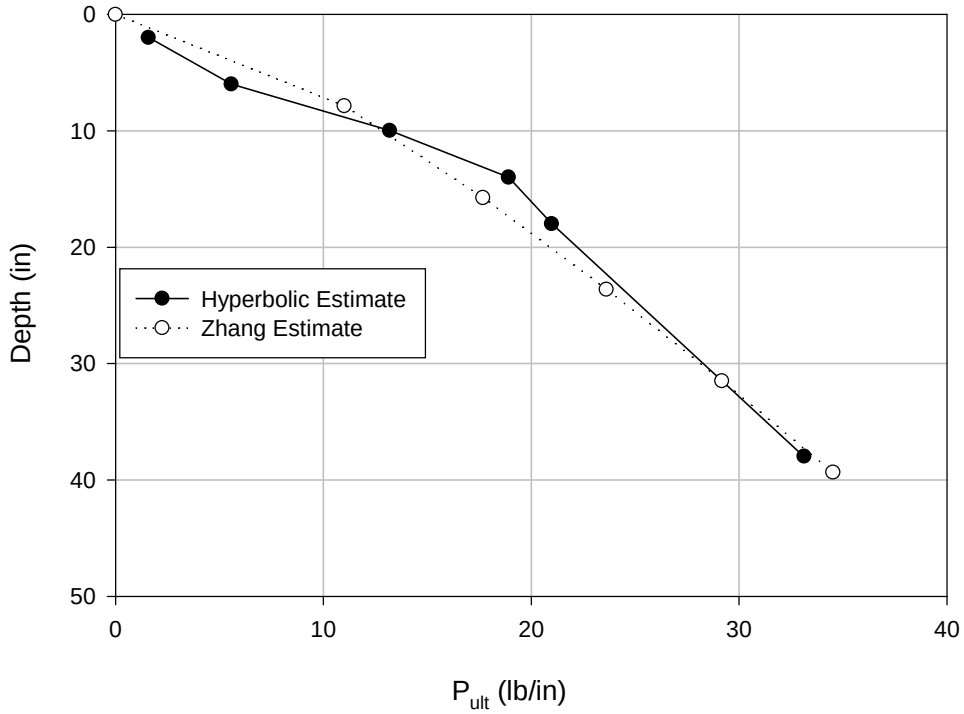

Figure 35 Hyperbolic vs Zhang

These results indicate a close match. This failure criterion and estimation procedure for P_{ult} will be later applied to the full-scale test results.

5.4 Comparison with Field Test Results

The k_{ho} and P_{ult} relationships were compared with the field test results from full-scale load tests in Caldwell and Wilson Counties in the following section. The laboratory values and the field values were divided by the width of the member to convert the subgrade reaction, k_h to the subgrade modulus coefficient, k_{ho} Also, a dimensionless depth value was obtained by dividing the embedded length, L, by the diameter, D, of the shaft for the laboratory and field results. A plot of L/D vs k_{ho} is shown in Figure 36.

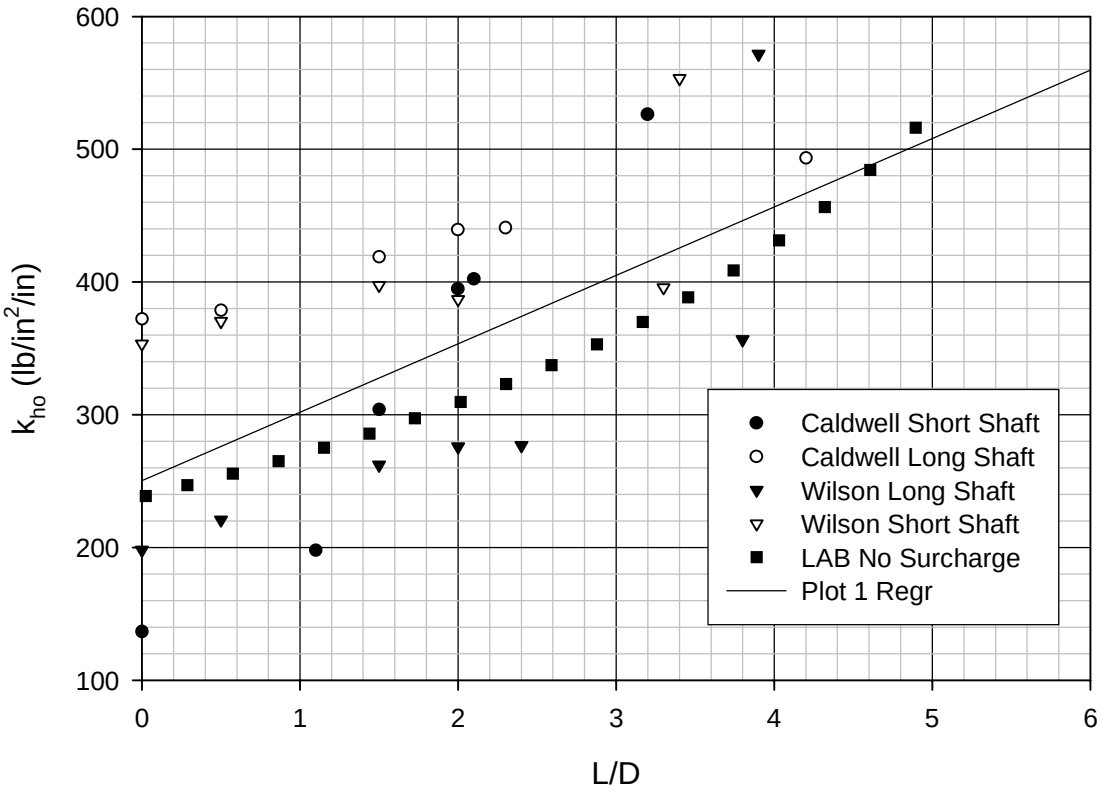

Figure 36 k_{ho} vs Depth for Field Results and Laboratory Testing

Based on Figure 36, a linear relationship can be used to estimate the variation of k_{ho} with depth. To create a method to estimate the field values of k_{ho}, a linear regression line was drawn through the data points and is represented by the following equation:

$$y = 51.5x + 250 \quad (26)$$

where x = Length/Diameter Ratio and,
y = k_{ho} (lb/in^2/in)

The R^2 value of 0.53 this indicates that the fitted curve does not fit the data particularly well, however, given the scatter of the data values and the relative location of the trend line, the author feels this is a reasonable estimate. As additional testing values are

added to the database, the general fit, R^2, of the curve should improve. This indicates that the laboratory testing conducted in the ABC mixture yields similar values to those found in the field. However, the spread of the points relative to the trend line also indicate that variances likely exist among the weathered rock types and have inherent installation effects.

To see the effect of the surcharge data, Figure 37 was constructed without a regression line. These results indicate that an increase in the confining stress creates a material that is actually stiffer than the weathered rock tested thus far.

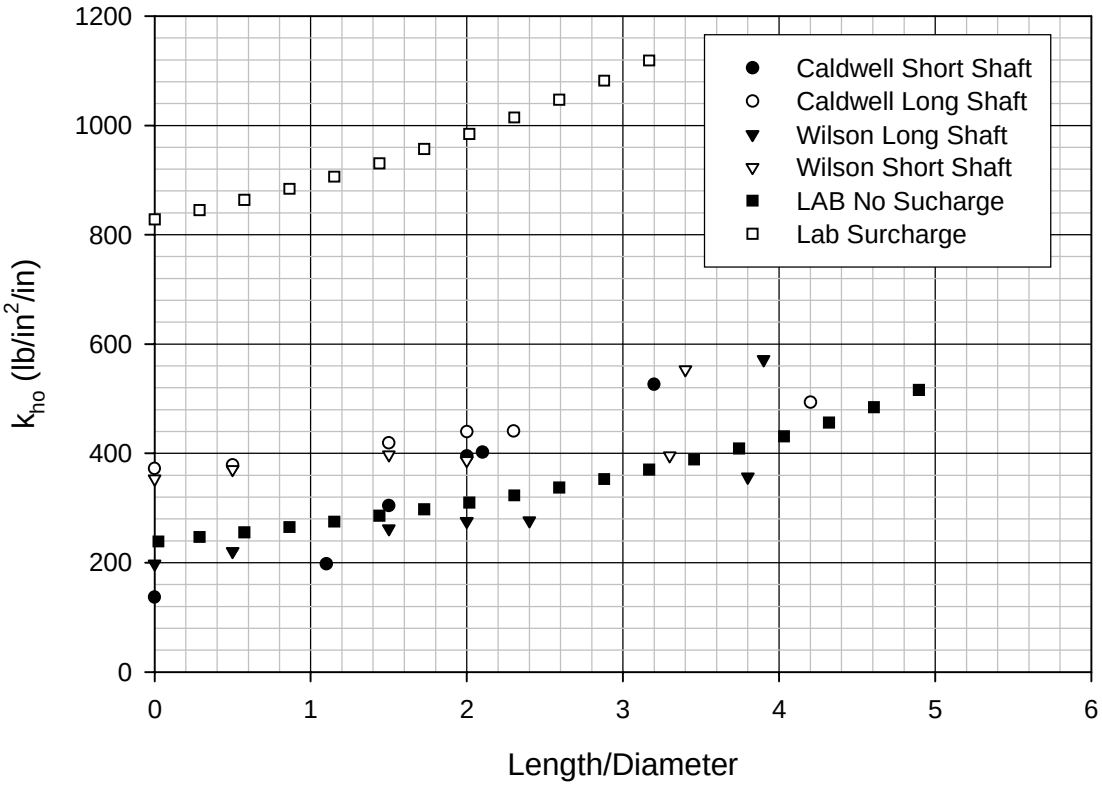

Figure 37 Both Lab Tests contrasted with Field Data

To estimate the values of P_{ult} between the laboratory and field, many comparisons were attempted, however a simple correlation could not be rationally developed. Thus the method proposed by Zhang et al (2000) is used again as an estimation for field P_{ult} results. The following parameters were used in this evaluation of the full-scale field test and the results are shown in Figure 38.

Table 9 Parameters for Estimation of P_{ult}

Property	Value
GSI	10
m_i	33
s	0
a	0.5
σ_c	60 Mpa

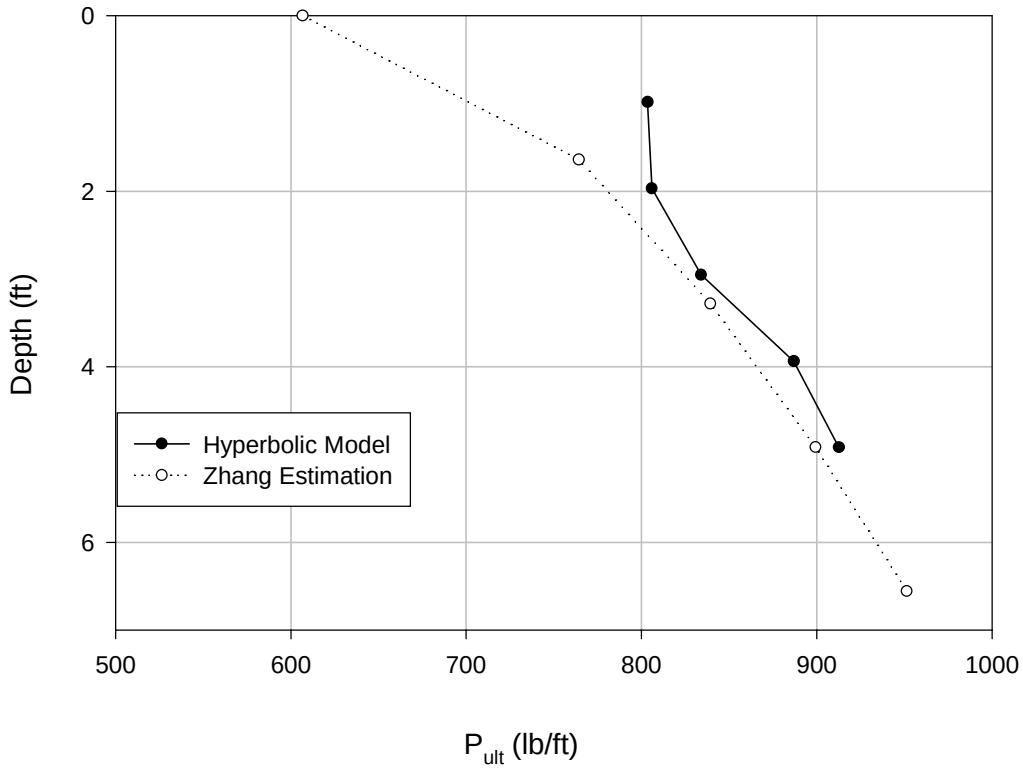

Figure 38 Full Scale Field Test vs Zhang Estimation

Again a close fit is seen. It is the opinion of the author that the P_{ult} can be reasonably estimated using the relationships presented here.

The benefits of approximating k_{ho} become apparent when comparing the methods proposed by Reese (1997) for weathered rock and Terzaghi (1955) for stiff clays, which are often used in design. To compare these methods, the following parameters will be used and the subgrade modulus, k_h will be evaluated:

Table 10 Comparison Parameters

Pile Diameter(ft)	E_{ir}* (psi)	Su (psf)
3.5 inches = .291 ft	347.5	1200

* This value is interpolated from the modulus values obtained in section 3.3 for a density of 125 pcf

Reese suggested using the following equations, as discussed previously. These are repeated here for convenience only

$$K_{ir} = k_{ir}E_{ir} \quad (5)$$

where, E_{ir} = initial modulus of rock and,
k_{ir} = dimensionless constant

$$k_{ir} = (100 + 400x_r/3b); \qquad 0 \le x_r \le 3b \quad (7)$$
$$k_{ir} = 500; \qquad x_r \ge 3b \quad (8)$$

Evaluating to a depth of ten feet, a distribution for k_{ho} can be determined. Also using the values in Table 10, a distribution for stiff clay can be determined. According to Terzaghi (1955), he recommended the subgrade reaction, k_h, be held constant with depth as shown in Figure 39.

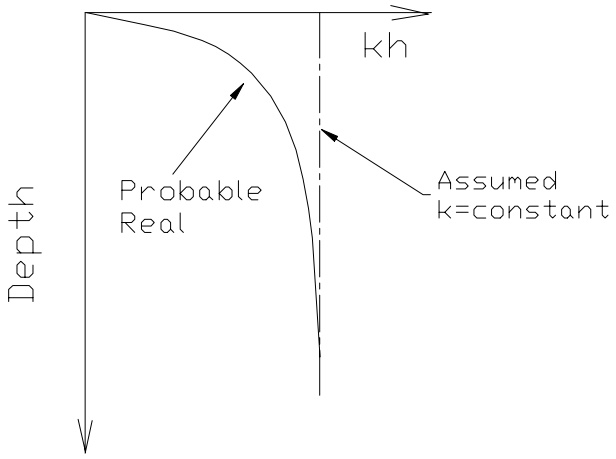

Figure 39 Variation of subgrade modulus with depth for stiff clays (Terzaghi, 1955)

Davisson (1970) recommended the following equation for the subgrade modulus in cohesive soils.

$$k_s = 67S_u \qquad (27)$$

where S_u is the unconfined shear strength (psi).

In Figure 40, it is noted that Reese's method greatly overshadows the clay model. To compare these values with the model I have proposed, I will look at an L/D value equal to 5 and evaluate this with the proposed equation.

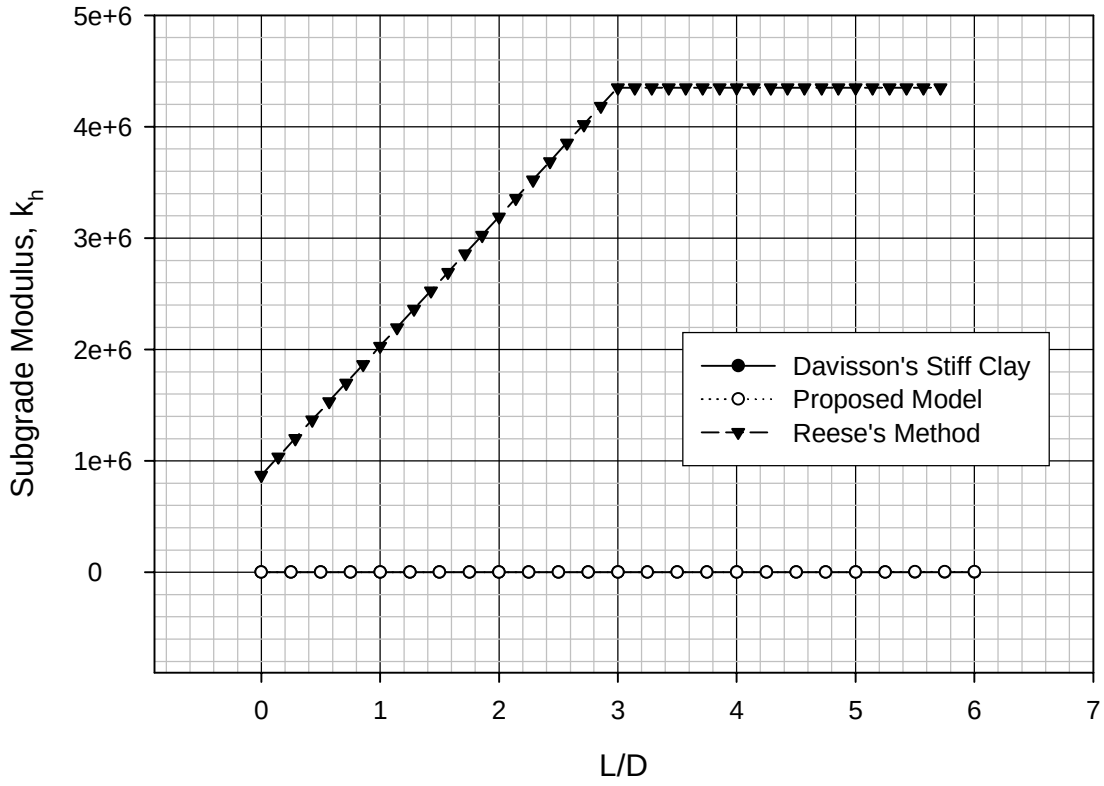

Figure 40 Reese vs Stiff Clay

For a given L/D = 5, the corresponding k_{ho} is equal to 507.5 lb/in^2/in. For a 3.5 in diameter pile, this correlates to a subgrade reaction of 1776.25 lb/in^2, which falls between the two curves in Figure 40, thus indicating that Reese's method overpredicts the initial modulus for weathered rock and the clay model underpredicts this same value. Figure 41 shows the proposed equation and the Stiff Clay values; Reese's Method has been removed to allow the comparison to be seen.

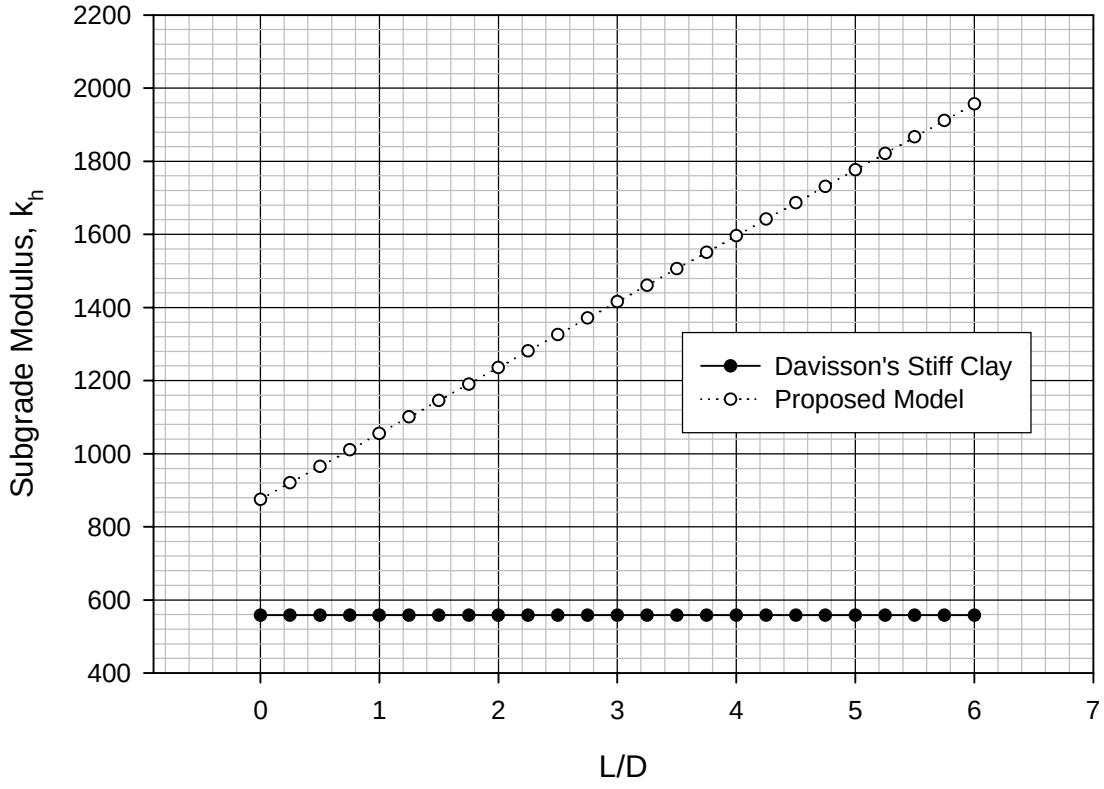

Figure 41 Proposed Equation compared with the Stiff Clay Equation

Based on the analysis and comparison, the proposed model for the subgrade coefficient produces a more reasonable, yet conservative value for the subgrade reaction, k_h, when analyzing weathered rock.

6.0 SUMMARY AND CONCLUSIONS

Research work is conducted to investigate the possibility of using laboratory model tests to simulate lateral response of drilled shafts embedded in soft weathered rock and discern their P-y curve function. Eight lateral load tests on instrumented model piles embedded in an Aggregate Base Course (ABC) medium are performed to evaluate the P-y curves. The ABC material is selected to simulate the response of soft weathered rock encountered in the field. The laboratory-evaluated P-y curves are compared to data from full-scale field tests performed in weathered rock. The two key parameters evaluated are the coefficient of subgrade reaction (k_{ho}) and the ultimate lateral resistance (P_{ult}). A distribution of k_{ho} with applied confining stress is evaluated and compared to results from procedures proposed by Reese (1997) for weathered rock and Terzaghi (1955) for stiff clay. A relationship developed for the distribution of subgrade modulus as a function of depth compared well with field data. The relationship of P_{ult} with depth as a function of Geological Strength Index (GSI) and friction angle is also presented. All results are viewed in the context of the field-measured response. Based on the results of this study, the following conclusions are advanced:

Results indicated that a hyperbolic P-y function seems to best represent the measured laboratory P-y curves.

- Model piles can be used to develop correlations that closely model full-scale conditions occurring in weathered rock masses.
- Aggregate Base Course will behave in a similar fashion to weathered rock.

- A comparison between laboratory and field data indicated that the ABC testing medium appears to yield k_{ho} and P_{ult} that behave in a fashion similar to weathered rock material. Accordingly, it seems that, when appropriately mixed, ABC can be used to model SWR encountered in the field.
- P_{ult}, when approximated using the Hoek-Brown failure criterion, closely approximates the P_{ult} derived from they Konder hyperbolic models.

RECOMMENDATIONS FOR FUTURE RESEARCH

Based on the results of this model study, the following recommendations are proposed for future research:

- Explore the dependence of P_{ult} on embedment by experimenting with different degrees of embedment.
- Evaluate further the use of surcharging to simulate surface confinement and its effects on k_{ho} and p_{ult}.
- Apply the proposed correlations to future field tests to validate their predictions.
- Further study the insitu rock masses for the effects of bonding and/or cohesion.
- Establish correlations to construct P-y curves for the soft weathered rock from the measured in situ lateral modulus using the rock dilatometer.

REFERENCES

Gabr, M., and Borden, R. H., 1992, Lateral Analysis of Piers on Sloping Profiles, Closure, Journal of Geotechnical Engineering, V. 118(6), pp. 969-972.

Gabr, M., 1993, Analysis of Laterally Loaded Shafts in Rock, Discussion of Paper by Carter and Kulhawy, Journal of Geotechnical Engineering, ASCE, 119 (12), pp. 2015-2018.

Briaud, J-L, 1992, The Pressuremeter, A. A. Balkema, Rotterdam, Netherlands.

Horton, J.W., 1991, The Geology of the Carolinas : Carolina Geological Society Fiftieth-Anniversary Volume, University of Tennesse.

Matlock, H., Bogard, D., and Lam, I. P., 1981, A Computer Program for the Analysis of Beam-Columns under Static Axial and Lateral Loading, University of Texas, Austin, Texas.

Poulos, H. G., 1971, Behavior of Laterally Loaded Piles: I – Single Piles, Journal of Soil Mechanics and Foundations, ASCE, 97(5), pp. 711-731.

Reese, L. C., and Welch, R. C., 1975, Lateral Loadings of Deep Foundation in Stiff Clay, Journal of Geotechnical Engineering, ASCE, 101(7), pp. 633-649.

Reese, L. C., 1997, Analysis of Laterally Loaded Piles in Weak Rock, Journal of Geotechnical and Geoenvironmental Engineering, ASCE, v 123 (11) Nov., ASCE, pp. 1010-1017.

Rocktest Limited, 1999, Dilatometer Model Probex-1 Instruction Manual, Rocktest Inc., Plattsburgh, New York.

Carter, J. P., Kulhawy, F. H., 1992, Analysis of Laterally Loaded Piles in Rock, Journal of Geotechnical Engineering, ASCE, Vol. 118 (6), ASCE, pp. 839-855.

Coates, D. F., 1970, Rock Mechanics Principles, Department of Energy Mines and Resources, Mine Branch Monograph, pp. 874.

Coon, R. F. and A. H. Merrit, 1970, Predicting Insitu Modulus of Deformation Using Rock Quality Indexes, Determination of the Insitu Modulus of Deformation of Rock, ASTM STP 477, pp. 154-173.

Digioia, A. M. Jr., Rojas-Gonzalez, L. F., 1994, Laterally Loaded Rock-Socketed Foundation, IEEE Transactions on Power Delivery, v 9 (3) Jul 1994 USA pp. 1570-1576.

Goodman, R. E., Van, T. K., and Heuze, F. E., 1968, The Measurement of Rock Deformability in Boreholes, Proc. 10th Symp. On Rock Mechanics, AIME, Austin, TX, pp. 523-555.

Hoek, E., and Bray J., 1981, Rock Slope Engineering 3rd Edition, The Institution of Mining and Metallurgy, London, U.K., pp. 100.

Hoek, E., and Brown, E.T., Practical Estimates of Rock Mass Strength, Int. J. Rock Mech. min.Sci., Vol 34, No. 8, pp. 1165-1186, 1997.

Kulhawy F. H., Trautmann C. H., and O'Rourke T. D., 1991, Soil Rock Boundary: What Is It and Where Is It?, Geotechnical Special Publication No. 28, ASCE, pp. 1-15.

Matlock, H, 1970, Correlations for Design of Laterally Loaded Piles in Soft Clay, Proc. 2nd Offshore Technology Conf., Vol. 1, pp. 577-594.

Mattlock, H., "Correlations for Design of Laterally Loaded Piles in Soft Clay", Paper no. OTC 1204, Offshore Technology conference, Dallas, Texas. 1970.

Poulos, H. G., and Davis, E. H., 1980, Pile Foundation Analysis and Design, Wiley, New York.

Reese, L. C., Cox, W. R., Koop, F. D., 1974, "Analysis of Laterally Loaded Piles in Sand", Paper No. 2080, Offshore Technology Conference, Dallas, Texas. 1974.

Reese, L. C., Cox, W. R., Koop, F. D., 1975, Field Testing and Analysis of Laterally Loaded Piles in Stiff Clay, Paper No. 2312, Offshore Technology Conference, Dallas, Texas.

Smith, R. E., Gabr, M. A., and Kula, J. R., 1991, Soil-Rock Transition Zone: Uncertainties for Design and Construction, Geotechnical Special Publication No. 28, ASCE, pp. 91-106.

Sowers,G.F., and Richardson, T. L., 1983, Residual Soils of Piedmont and Blue Ridge, Transportation Research Record 919, Transportation Research Board, Washington D. C.

Davisson, M.T., 1963, "Estimating Buckling Loads for Piles", Proceedings of the Second Pan American Conference on Soil Mechanics and Foundation Engieering, Vol. I, pp. 351-369.

Terzaghi, K., 1955, "Evaluation of Coefficiant of Subgrade Reaction,", Geotechnique, Vol. 5, No. 4, pp. 297-326.

Zhang, L., Ernst, H., and Einstein, H., Nonlinear Analysis fo Laterally Loaded Rock-Socketed Shafts, Journal of Geotechnical and Environmental Engineering, November 2000.